

Proline hydroxylase 2 (PHD2) promotes brown adipose thermogenesis by enhancing the hydroxylation of UCP1



Fan Li¹, Fenglin Zhang¹, Xin Yi¹, Lu Lu Quan¹, Xiaohua Yang¹, Cong Yin¹, Zewei Ma¹, Ruifan Wu¹, Weijie Zhao¹, Mingfa Ling¹, Limin Lang¹, Abdelaziz Hussein¹, Shengchun Feng¹, Yiming Fu¹, Junfeng Wang¹, Shuyi Liang¹, Canjun Zhu¹, Lina Wang¹, Xiaotong Zhu¹, Ping Gao¹, Qianyun Xi¹, Yongliang Zhang¹, Lin Zhang¹, Gang Shu¹, Qingyan Jiang^{1,**}, Songbo Wang^{1,2,*}

ABSTRACT

Objective: Brown adipose tissue (BAT) plays a crucial role in regulating non-shivering thermogenesis under cold exposure. Proline hydroxylases (PHDs) were found to be involved in adipocyte differentiation and lipid deposition. However, the effects of PHDs on regulatory mechanisms of BAT thermogenesis are not fully understood.

Methods: We detected the expression of PHDs in different adipose tissues by using immunoblotting and real-time PCR. Further, immunoblotting, real-time PCR, and immunostaining were performed to determine the correlation between proline hydroxylase 2 (PHD2) and UCP1 expression. Inhibitor of PHDs and PHD2-sgRNA viruses were used to construct the PHD2-deficiency model in vivo and in vitro to investigate the impacts of PHD2 on BAT thermogenesis. Afterward, the interaction between UCP1 and PHD2 and the hydroxylation modification level of UCP1 were verified by Co-IP assays and immunoblotting. Finally, the effect of specific proline hydroxylation on the expression/activity of UCP1 was further confirmed by site-directed mutation of UCP1 and mass spectrometry analysis.

Results: PHD2, but not PHD1 and PHD3, was highly enriched in BAT, colocalized, and positively correlated with UCP1. Inhibition or knockdown of PHD2 significantly suppressed BAT thermogenesis under cold exposure and aggravated obesity of mice fed HFD. Mechanistically, mitochondrial PHD2 bound to UCP1 and regulated the hydroxylation level of UCP1, which was enhanced by thermogenic activation and attenuated by PHD2 knockdown. Furthermore, PHD2-dependent hydroxylation of UCP1 promoted the expression and stability of UCP1 protein. Mutation of the specific prolines (Pro-33, 133, and 232) in UCP1 significantly mitigated the PHD2-elevated UCP1 hydroxylation level and reversed the PHD2-increased UCP1 stability.

Conclusions: This study suggested an important role for PHD2 in BAT thermogenesis regulation by enhancing the hydroxylation of UCP1.

© 2023 The Authors. Published by Elsevier GmbH. This is an open access article under the CC BY-NC-ND license (<http://creativecommons.org/licenses/by-nc-nd/4.0/>).

Keywords PHD2; UCP1; Hydroxylation; BAT thermogenesis

1. INTRODUCTION

Brown adipose tissue (BAT) plays a vital role in maintaining energy homeostasis and body temperature through its uncoupling respiration [1–3]. Uncoupling protein 1 (UCP1), the proton leak channels abundantly located in BAT mitochondria inner membrane, is a crucial factor affecting BAT function [4,5]. UCP1 deficiency leads to the dysfunction of the cellular mitochondrial respiratory chain and impairs the body's energy consumption severely [6–8]. Thus, the expression and activity of UCP1 are limiting factors in BAT thermogenesis and energy homeostasis. Post-translational modification (PTM) modifies the amino acid residues on the protein, and affecting its function and activity [9–11]. Recently,

UCP1 has been demonstrated to be modified in a variety of ways, including sulfenylation, succinylation, phosphorylation, and ubiquitination, indicating the important role of PTM in regulating UCP1 expression or activity [12–15]. However, research on the PTM of UCP1 still scarce and it is unclear whether other PTM modulate UCP1.

Proline hydroxylases (PHDs) belong to an oxygen and α -ketoglutarate dependent dioxygenase containing three major members: PHD1, PHD2, and PHD3. PHDs can affect the stability and function of the target proteins through hydroxylating specific proline residues [16,17]. As the classical regulatory substrate of PHDs, HIF α (Hypoxia induce factor α) can be hydroxylated by PHDs and then degraded by the protein ubiquitination pathway mediated by E3 ubiquitin ligase. On the

¹Guangdong Provincial Key Laboratory of Animal Nutrition Control and National Engineering Research Center for Breeding Swine Industry, College of Animal Science, South China Agricultural University, Guangzhou 510642, PR China ²Yunfu Branch, Guangdong Laboratory for Lingnan Modern Agriculture, Wen's Foodstuffs Group Co., Ltd, Yunfu 527400, PR China

*Corresponding author. Guangdong Provincial Key Laboratory of Animal Nutrition Control and National Engineering Research Center for Breeding Swine Industry, College of Animal Science, South China Agricultural University, Guangzhou 510642, PR China. E-mail: songbowang@scau.edu.cn (S. Wang).

**Corresponding author. E-mail: qyjiang@scau.edu.cn (Q. Jiang).

Received February 10, 2023 • Revision received May 30, 2023 • Accepted May 31, 2023 • Available online 4 June 2023

<https://doi.org/10.1016/j.molmet.2023.101747>

contrary, when exposed to hypoxia, the activity of PHDs is extremely inhibited and HIF α is thus continuously activated [17–19]. Therefore, PHDs have been widely studied as intracellular oxygen receptor proteins.

However, recent studies have confirmed that PHDs participate in the regulation of other protein activity and function in a hydroxylation-modified way besides HIF α , including AKT [20], FoxO3 [21], p53 [22], PKM2 [23], ACC2 [24], CPT1B [25], and TFAM [26]. The hydroxylation modification of these proteins showed the universal and extensive roles of PHDs in regulating protein functions. Additionally, it has been clarified that PHDs took part in physiological processes such as adipocyte differentiation, adipose deposition, and mitochondrial fatty acid oxidation. For example, PHDs could inhibit the expression of anti-adipogenic factors and promote PPAR γ expression during adipogenesis [27]. PHD2 knockout promotes adipose expansion by suppressing lipolysis [28]. Besides, PHD2/PHD3 can directly combined with CPT1B to promote mitochondrial fatty acid utilization and oxidation [25]. These revealed the important role that PHDs may play in the process of adipose metabolism. However, whether PHDs-induced hydroxylation is involved in BAT thermogenesis remains largely unknown.

In the present study, PHD2 was found highly expressed in BAT, colocalized with thermogenic protein UCP1, and its expression level was positively correlated with UCP1. Meanwhile, inhibition or knockdown of PHD2 in vitro or in vivo all resulted in impairment of BAT thermogenesis. Mechanistically, PHD2 directly bound to UCP1 protein, regulated the hydroxylation of proline residues on UCP1, and affected the stability of UCP1 protein, while mutation of the specific prolines in UCP1 eliminated the effects of PHD2. Overall, our research demonstrated that PHD2 promoted brown adipose thermogenesis by enhancing the hydroxylation of UCP1, and providing the new regulatory target for UCP1 activity and BAT thermogenesis.

2. MATERIALS AND METHODS

2.1. Animals

The study was approved by the College of Animal Science, South China Agricultural University. All experiments were conducted following The Instructive Notions with Respect to Caring for Laboratory Animals (Ministry of Science and Technology, Beijing, China). Wild-type 4-week-old C57BL/6 J male mice were obtained from the Animal Experiment Center of Guangdong Province [permission SYXK (Yue) 2019-0136], and all animals were group housed in the animal facility with ad libitum access to food and water pre-feeding-for-2-weeks. Randomized grouping all according to the weight of mice. The room was temperature-controlled at 24 ± 1 °C with 60%–70% humidity under a 12-hour light/dark cycle room.

Packaging and injection of PHD2-sgRNA virus were referred to previous steps [29,30] with modifications. PHD2 knockdown mice were generated by in-situ injecting AAV9-CAS9 virus combined with AAV9-U6-PHD2-sgRNA virus or AAV9-U6-scramble-sgRNA virus (abm, Canada, 1×10^{12} pfu/ml) in BAT. The validated sgRNA sequence for PHD2 knockdown is target1: CGGCAGTACTGCGAGCTGTG, target2: ATGGAGAACCTGCTGCGCTG, and target3: CACAAGCTGGTGTGCCAGGG. The given viruses were directly injected with 3 points into BAT of the 6-week-old mice (100 μ L/dose, 5×10^{11} pfu/ml, sterile saline dilution). The body weight and food intake were recorded weekly for 4 weeks, starting formally the two weeks after virus injection and infection. For HFD treatment, mice were fed a diet containing 60% fat-derived calories (Dyets Diet, HF60) to induce obesity model, two mice per cage, the average food intake was recorded by cage, and the weight of mice

was calculated by the single animal. All animals were anesthetized with isoflurane for sampling.

2.2. Isolation of stromal vascular fraction (SVF) from iBAT

Primary stromal vascular fraction (SVF) cells were isolated from the BAT of 3-week-old male C57BL/6 J mice as previously described [31,32] with modification. BAT was minced into pieces with scissors and digested using collagenase I (2 mg/ml, 17100017, Gibco, containing 3 mM CaCl₂) at 37 °C water bath for 30 min. Tissue homogenates were filtered through 40 μ m mesh to remove undigested tissues, followed by centrifugation at 800g for 5 min. Resuspended pellets containing SVF cells were incubated with pre-cooled red blood cell lysate buffer for 5 min, then collected by centrifugation at 600g for 5 min and suspended with DMEM/F12 (Gibco) supplemented with 10% fetal bovine serum (FBS) (Gibco), penicillin (100 U/ml) and streptomycin (100 mg/ml, Thermo Fisher Scientific). The cell suspension was seeded in 25 cm² cell culture plates and cultured at 37 °C with a 5% CO₂ humidified incubator. The medium was changed every other day. The SVF cells with less than 4 passages were used for brown adipocyte differentiation in vitro.

2.3. Brown adipocyte differentiation and PHD2-knockdown adenovirus transfection

Brown adipogenic differentiation of SVF was carried out as a previous procedure [31] with modification. Briefly, 48 h post SVF cells confluence, DMEM/F12 induced medium containing 5 μ g/mL insulin (Beyotime), 0.5 mM 3-isobutyl-1-methylxanthine (Sigma), 125 μ M indomethacin (Sigma), 1 μ M dexamethasone (Sigma) and 1 nM 3,3,5-Triiodo-L-thyronine (T3 Sigma) with 10% FBS was added to cultured cells for 48 h. Then, cells were cultured in the maintenance medium containing 5 μ g/ml insulin and 1 nM T3 until the sixth day, with the change of medium every other day. To activate thermogenic gene expression, fully differentiated brown adipocytes were treated with isoproterenol (10 μ M, Sigma) for 24 h before harvest.

For PHD2-knockdown in vitro, CAS9 and PHD2-sgRNA (target1: CGGCAGTACTGCGAGCTGTG, target2: ATGGAGAACCTGCTGCGCTG, and target3: CACAAGCTGGTGTGCCAGGG) (abm, Canada, 1×10^{11} pfu/ml) were packaged into adenovirus for primary cells infection. When reached about 30%–40% confluence, the cells were added to DMEM/F12 medium containing adenovirus (MOI = 1:400) and 10% FBS and incubated for 12 h. Then the fresh DMEM/F12 medium was added and GFP fluorescence was observed 48 h after transfection. Afterward, the cells were induced brown adipogenesis according to the above-mentioned methods.

2.4. RNA interference by siRNA

RNA interference was conducted as previously described [33]. 24 h after PHD2-knockdown adenovirus infection. SVF cells were grown to a 60–70% confluent ratio before siRNA transfection. 100 nM of the small interfering RNA (siRNA) targeting HIF-1 α (siRNA: sense 5' UGUGAGCU-CACAUCUUGAUTT 3'; antisense 5' AUCAAGAUGUGAGCUCACATT 3') or siRNA control (GenePharma, Shanghai, China) were transfected to cells using the lipofectamine RNAiMAX (Invitrogen, USA) reagent according to the manufacturer's instructions. Then, the cells were differentiated according to the above differentiation methods after confluence.

2.5. Medium pH and lactate content measurements

The pH spear tester (ThermoFisher) was used to detect medium pH after PHD2 knockdown and HIF-1 α interference in brown differential adipocytes. Then medium lactate content was measured by lactate

assay kit (A019-2-1, Nanjingjiancheng bioengineering institute, China) according to the manufacturer's instructions.

2.6. PHD2 inhibition

For PHDs inhibition *in vivo*, DMOG (40 mg/kg, PHD-pan inhibitor, MCE) was intraperitoneally (i.p) injected into mice at 8-week-old, then the mice were treated with 4 °C cold stimulation for 8 h and the body temperature was detected. *In vitro*, 300 μM DMOG (MCE) was added to the induced medium to treat primary adipocytes until six days.

2.7. Adipose tissue section and histology analysis

The mice were sacrificed, and the adipose tissues were separated and harvested. The BAT of wild-type mice was frozen by liquid nitrogen and embedded with OCT (TissueTek), then sliced into 15 μm in thickness by the freezing microtome (CM1950, Leica, Germany) for further immunofluorescence staining, the whole embedding and slicing process was kept at −35 °C. For histological analysis, the BAT of HFD-fed PHD2-KD mice was harvested, trimmed, and immersed in a special fixative for adipose tissue (BioFAVOR, Wuhan, China). Tissues embedded in paraffin were sectioned into 5 mm in thickness, followed by deparaffinization, rehydration, and hematoxylin and eosin (H&E) staining as previous paper [34,35].

2.8. Immunocytochemistry and immunofluorescence staining

For immunofluorescence staining of brown differential adipocytes, the cells were inoculated into 6-well plates with poly-lysine (0.1 mg/ml, Solarbio) coated slides. When the cells were fully differentiated, take out the glass cell slide. Then cell slides and adipose frozen sections obtained above were fixed with pre-cooled methanol and acetone (1:1 mixture) for 20 min at 4 °C as in previous research [36], washed with phosphate-buffered saline (PBS) for three times at 5 min per time, blocked with blocking buffer including 2% BSA/5% normal goat serum/0.1% sodium azide/PBS for 30 min at room temperature, and incubated with primary antibodies overnight at 4 °C. Antibodies used included rabbit anti-UCP1 (14670S, CST), mouse anti-PHD2 (ab103432, abcam). Subsequently, sections were washed in PBS three times for 5 min per time, incubated with goat anti-mouse IgM/Alexa Fluor 555 antibody (bs-0368G-AF555, Bioss), goat anti-mouse FITC antibody (bs-50950, Bioworld), goat anti-rabbit FITC antibody (bs0295G-FITC, Bioss), and goat anti-rabbit Alexa Fluor 555 antibody (bs-0295G-AF555, Bioss) in a dilution ratio of 1:1000 with PBS for 1 h. Then, sections were suppressed background for 5 min with 0.05% Sudan black diluted with 70% hexanol and sealed with an anti-fluorescence quenching agent (0100-01, SouthernBiotech). Finally, Nikon Eclipse Ti-S Microscope was used to take fluorescent pictures. Fluorescence intensity statistics were quantified by image J.

2.9. Oil-red staining

For brown differential adipocyte staining, the procedures were performed as the previous description [33], cells were washed twice with PBS and fixed with 4% paraformaldehyde for 30 min at room temperature. Afterward, cells were stained with a filtered Oil Red O solution (0.5% Oil Red O in isopropyl alcohol) for 1 h at room temperature, washed several times with distilled water, then observed and photographed by the stereoscope. Finally, the Oil Red O was eluted with isopropanol and the eluted buffer was collected. The 520 nm absorbance value of the eluted buffer was detected and measured by a microplate reader (BioTek).

2.10. Quantitative real-time PCR

Total RNAs were extracted from primary cells and mouse adipose tissue samples by using an RNA extraction kit (Magen BioSciences) according to the manufacturer's instructions. By treated with gDNA remover (EZBioscience, A0010CGQ), 2 μg of total RNA was reverse transcribed to cDNA in a final 20 μL using 4 × RT Master Mix (EZBioscience, A0010CGQ) according to the manufacturer's instructions. Then, total cDNA/Sense and antisense primers/SYBR Green Real-Time PCR Master Mix reagents (EZBioscience, A0001-R2)/Nucleic acid-free water were mixed for Real-Time quantitative PCR. The quantitative PCR was performed with the Applied Biosystems QuantStudio 3 Real-Time PCR System (Thermo Fisher Scientific, USA). The related gene primers were synthesized in Shanghai Sangon Biotech according to Table 1.

2.11. Absolute quantitative PCR analysis

The absolute quantitative PCR assay was performed according to the previous study [35,37] to determine the gene copy number of PHDs in different adipose tissues. Briefly, the cDNA samples were obtained in relatively quantitative RT-PCR analyses. The specific PCR amplification product was purified by electrophoresis and gel extraction using an Agarose Gel Recovery kit (D2111-02; Magen BioSciences) to generate a standard curve for genes. Then DNA concentration was detected by NanoDrop (2000c; Thermo Fisher Scientific). The absolute copy number of each sample was calculated according to the following formula: $C = A/B \times 6.02 \times 10^{14}$. A: DNA concentration obtained by OD 260 analysis (μg/μl); B: the molecular weight of the synthesized DNA (Daltons); C: copy number of the synthesized DNA (copies/μl). Subsequently, serial dilution was carried out on each purified PCR product and used as templates for quantitative real-time PCR to the target gene. Then Ct value of each dilution was obtained, and the standard curve of each gene was plotted as a linear regression of the copy number versus Ct values. Finally, The Ct value of each gene was calculated and quantification data of the genes were counted by interpolating the Ct value into the standard curve.

2.12. Protein extract and immunoblotting analysis

To detect the expression level of the target proteins by immunoblotting analysis. A total protein extraction kit (APPLYgen, P1250) and RIPA lysis

Table 1 — Primer sequences used for qRT-PCR.

Gene	Forward primer sequence (5'–3')	Reverse primer sequence (5'–3')
<i>PHD1</i>	ACCAGGCCCTTTGACCTCAAGAAA	TCTTGTGCAACTGGGTGGTTC
<i>PHD2</i>	AGTCCCAGGTCAACAAGCTG	TTTCTCCTGTCACTCTCAACA
<i>PHD3</i>	TCCTGCACCCCGATTTACTT	CTTTATGGGTGAAGGCTGGC
<i>UCP1</i>	TTGGGCTTCTATGCTGGGAG	GTGAATGCTATGCTCTTCTGTCT
<i>Dio2</i>	CTGTTGCGATTGATGTGGCT	CCCACCACTCTCTGACTTT
<i>PGC-1α</i>	AAGTGTGGAACCTCTCTGGAAGCTG	GGGTTATCTTGGTTGGCTTTATG
<i>PGC-1β</i>	TCCTGTAAAAGCCCGAGTAT	GCTCTGGTAGGGGCACTGA
<i>Cidea</i>	ATCACAACCTGGCCTGGTTACG	TACTACCCGGTGTCCATTCT
<i>PPARγ</i>	GGAAGACCACTCGATTCCCTT	GTAATCAGCAACCATTGGGTCA
<i>β-actin</i>	TAGGCGGACTGTTACTGAGC	AATCCTGAGTCAAAGCGCC

Note: PHD1, prolyl hydroxylase 1; PHD2, prolyl hydroxylase 2; PHD3, prolyl hydroxylase 3; UCP1, uncoupling protein 1; Dio2, deiodinase iodothyronine type II; PGC-1α, peroxisome proliferator-activated receptor γ co-activator1α; PGC-1β, peroxisome proliferator-activated receptor γ co-activator1β; PPARγ, peroxisome proliferator-activated receptor γ; Prdm16, positive regulatory domain containing16; Cidea, cell death inducing DFFA like effector A.

buffer (Bestbio, BB3201) were used to lyse adipose samples or brown differential adipocytes. The nuclear protein extraction kit (Bestbio, BB3112) and mitochondrial protein extraction kit (Bestbio, BB3176) were used to isolate nuclear or mitochondrial protein according to the procedure of the manufacturer's instructions (1 mM PMSF and protease inhibitor cocktail were added to protein lysates). The protein concentration was determined by bicinchoninic acid (BCA) protein assays (Thermo Fisher Scientific). When the sodium dodecyl sulfate (SDS)-polyacrylamide gel electrophoresis gels were finished, the proteins were transferred to PVDF membranes (EMD Millipore). Then, the PVDF membranes were incubated with the following primary antibodies: rabbit anti-Tubulin- β (AP0064; Bioworld Technology), rabbit anti- β -actin (AP0060; Bioworld Technology), rabbit anti-UCP1 (#14670; Cell Signaling), rabbit anti-PHD1 (A3730; ABclonal), rabbit anti-PHD2 (A14557; ABclonal), rabbit anti-PHD3 (A8001; ABclonal), rabbit anti-HIF-1 α (382600; ZENBIO), rabbit anti-PGC-1 α (NBP-1-04676SS; Novus Biologicals), rabbit anti-PPAR γ (#2443; Cell Signaling), mouse anti-Prdm16 (bsm-51634 M; Bioss antibodies), rabbit anti-COXIV (A6564; ABclonal), rabbit anti-VDAC1 (A19707; ABclonal), rabbit anti-HistoneH3 (#4499; Cell Signaling), rabbit anti-hydroxyproline (ab37067; Abcam) at 4 °C overnight. Followed by incubation with the appropriate secondary antibody like goat anti-rabbit and goat anti-mouse (Bioworld Antibodies) for 1 h at room temperature. The anti-tubulin and actin antibody was used at a 1:5000 dilution, other primary antibodies were used at a 1:1000 dilution. Protein levels were detected by a FluorChemistry fluorescent imaging system (Tanon-5200) and were analyzed by using ImageJ software (Image Processing and Analysis in Java; National Institutes of Health, Bethesda, MD, USA).

2.13. Co-immunoprecipitation (co-IP) and hydroxylation detection

Co-immunoprecipitation analysis was conducted as described previously [38]. UCP1 and PHD2 immunoprecipitation was performed with Protein A + G magnetic dynabeads (88803, Thermo Fisher Scientific) and anti-Flag magnetic dynabeads (P2115, Beyotime). Total cells or tissues were lysed in a buffer containing 20 mM Tris-HCl, 150 mM NaCl, 2 mM EDTA, 0.2 mM EGTA, 1% NP-40, 10% glycerol, 1 mM PMSF, and protease and phosphatase inhibitor cocktails. Lysates were incubated overnight with Protein A + G magnetic dynabeads which crossed the link with rabbit anti-PHD2 (A14557; ABclonal), rabbit anti-UCP1 (#14670; Cell Signaling), and Goat anti-rabbit IgG (#2729; Cell Signaling) or Flag magnetic dynabeads overnight at 4 °C in a vertical mixing rotator. Redundant extracts were used as input control. On the second day, dynabeads were washed with lysis buffer for three times, and collected by magnetic frame. Then dynabeads samples were eluted by boiling with 2 \times SDS-PAGE buffer and stored at -20 °C until immunoblotting assay. UCP1 immunoprecipitation protein was incubated with hydroxyproline antibody (OH-Pro) to detect UCP1 hydroxylation according to a published paper [24]. And mouse anti-rabbit IgG (L27A9; Cell Signaling) was used for secondary antibody incubation.

2.14. Simulative extracellular hydroxylation analysis

Simulative hydroxylation detection in vitro was proceed as shown in Figure 6C. Briefly, 293T cell protein lysates transfected with UCP1-GFP plasmid were incubated with protein A + G magnetic dynabeads linked with UCP1 antibody overnight. According to the previous description with modification [23,39], on the second day, the dynabeads were collected and incubated with 0.5 μ g and 1.5 μ g PHD2 plasmid transfected 293T cell lysates with equal amounts of protein in a reaction buffer containing 40 mM Tris-HCl (pH 7.4), 100 mM NaCl, 3 mM MgCl₂, 5 mM ascorbate, 1.5 mM FeCl₂, 4 mM α -ketoglutarate and 2 mg/ml BSA. The enzyme reaction was carried out at 37 °C for

30 min. Then dynabeads samples were washed and eluted by boiling with 2 \times SDS-PAGE buffer and stored at -20 °C until hydroxylation immunoblotting assay.

2.15. Mass spectrometry

For mass spectrometry, BAT of mice with 4 °C cold exposure for 5 days was collected. Then protein samples were resolved by SDS-PAGE followed by coomassie staining. Bands corresponding to UCP1 (Red box marking in SpFig. S5b) were excised and sent to Wininnovate Biotechnology Co. Ltd. in Shenzhen for protein hydroxylation identification.

The MS/MS data were analyzed for protein identification and quantification using PEAKS Studio 8.5. The targeted database search was against mouse UCP1 sequence (P12242) obtained from UniProtKB with a maximum of two missed cleavages for trypsin semi-specific digest mode to identify matched spectra. The following settings were selected: Oxidation (M), Acetylation (Protein N-term), Deamidation (NQ), Pyro-glu from E, Pyro-glu from Q, and hydroxylation (+15.9949 molecular weight [MW] shift) for variable modifications as well as fixed Carbamidomethylation of cysteine. Precursor and fragment mass tolerance was set to 10 ppm and 0.05 Da respectively.

2.16. Plasmids, lentivirus transfection, and UCP1 mutation

The plasmids UCP1-PCDH-GFP-PURO and PHD2-Flag-CMV-RFP-2A-PURO which expressed UCP1-GFP and PHD2-RFP respectively were constructed by inserting the corresponding cDNA into lentiviral vector between the Swal/EcoRI and EcoRV/XhoI sites (Fenghbio, China and abm, Canada). Following a previous research [40], the mUCP1-PCDH-GFP-PURO series which expressed mutation of UCP1 (Pro to Ala) targeting Pro33, Pro133, Pro232 were generated by quickmutation™ site-directed mutagenesis kit (Beyotime, China) according to the procedure of the manufacturer's instructions. The mutated sequences in UCP1 are Pro33, 5'-CAGATATCATCACCTTC*GCG*CTGGACA CTGCCAAAGT-3' and 5'-GTCTATAGTAGTGAAG*CGC*GACCTGTGACGG TTTCA-3'; Pro133, 5'-CAGTGTTCATTGGGGCAG*GCT*ACAGAGGTCGTGAAG G-3' and 5'-GTCACAAGTAACCCGTCGATGTCTCCAGCACTTCC-3'; Pro232, 5'-ACCACACTCCTGGCCTCT*GCA*GTGGATGTGGTAA-3' and 5'-TGGTGTGA GGACCGGAGA*CGT*CACTACACCATT-3'.

For HEK 293T cells plasmid transfection, opti-MEM reduced serum medium (Gibco) was used to dilute corresponding plasmid and lipofectamine 2000 (Invitrogen), then plasmids and lipofectamine 2000 medium were mixed and added into HEK 293T cells, and the high glucose medium with 10% FBS was changed after 6 h of transfection. 48 h after transfection, the fluorescence expression was observed and further studies were carried out.

For SVF cell transfection, UCP1-GFP, PHD2-RFP, and P133A UCP1-GFP plasmids were packaged into lentivirus (3 \times 10⁸ pfu/ml, OBIO Technology, Shanghai). According to the procedure of the manufacturer of virus infection and previous paper [41], when cells confluence reached about 30%–40%, lentivirus (MOI = 1:50) was added to DMEM/F12 medium with 10% FBS in the presence of polybrene (7 μ g/ml) and incubated with cells for 16 h, then the fresh DMEM/F12 medium was added to the cell hole. Fluorescence was observed 48 h after transfection. Then, the cells were differentiated according to the above differentiation methods after confluence.

2.16.1. Serum/plasma TG and NEFA measurements

The triglyceride (TG) and nonesterified free fatty acids (NEFA) content in mice serum/plasma were detected by TG assay kit (A110-1-1, Nanjingjiancheng bioengineering institute, China) and NEFA assay kit (A042-2-1, Nanjingjiancheng bioengineering institute, China) according to the manufacturer's instructions.

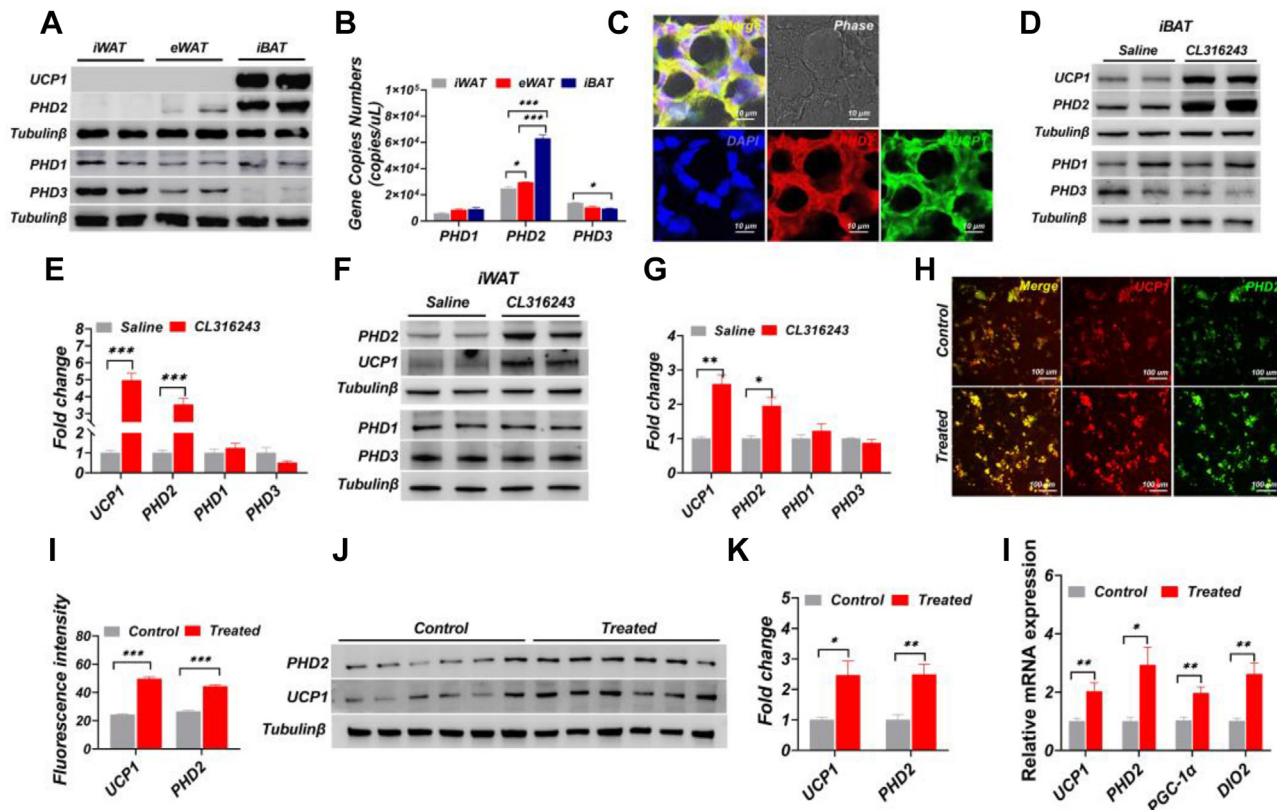


Figure 1: PHD2 expression was highly enriched in BAT, colocalized, and positively correlated with UCP1 expression. (A) PHDs and UCP1 protein expression in mice different adipose tissues (n = 4 per group). (B) The absolute quantification analysis of PHDs expression level in mice different adipose tissues (n = 6 per group). (C) Colocalization of PHD2 and UCP1 protein in mice BAT were determined by immunofluorescence staining. Scale bars, 10 μ m. d-g, C57BL/6 J mice were intraperitoneal (i.p.) injected with either vehicle or CL316243 (1 mg per kg) every other day for a week. Immunoblotting was performed (D, F), and protein (E, G) levels of PHDs and UCP1 were quantified in BAT and iWAT (n = 4 per group). H–L, Differentiated brown adipocytes of mice were treated with vehicle or 10 μ M isoproterenol for 24 h. The PHD2 and UCP1 immunofluorescence staining was performed (H) and quantification (n = 6 per group) (I). Scale bars, 100 μ m. Immunoblotting was performed (J) and quantification (n = 6 per group) (K) of PHD2, UCP1, and PGC-1 α protein were calculated. mRNA levels of PHD2, UCP1 and thermogenesis genes were determined (n = 6 per group) (L). All data are presented as means \pm SEM. All data points are biological replicates. Statistical analyses were performed by the two-tailed Student's t test between the individual groups. *P \leq 0.05, **P \leq 0.01 and ***P \leq 0.001 compared with the corresponding control group.

2.17. Cold exposure and body temperature monitoring

For acute cold exposure, mice were individually placed in cages at 4 $^{\circ}$ C for 8 h with free access to water only. 8 h later, the brown adipose temperature was monitored by infrared thermal detection (FLIR, America), and rectal temperature was detected by the anal thermometer.

2.18. Metabolic analysis

According to the previous procedure with modification [42], metabolic cage studies were conducted using Promethan Metabolic Screening Systems (Sable Systems International, North Las Vegas, NV, USA). After adaptation in metabolic cages for 5 days, CO₂, O₂ consumption, and locomotor activities were monitored formally starting at 18:00 (5 min/time for 24 h) with BAT-PHD2-KD mice fed by HFD. For PHD2 inhibition mice, metabolic dates were measured for 48 h. The first 24 h were used as a basic metabolic level, then DMOG and CL316243 were injected intraperitoneally into mice at 18:00 of the second day as arrow indicated in Figure 2H,J. And the monitor was conducted for another 24 h. Data were collected and analyzed by MetaScreen-Data Collection Software (V2.3.17) and Expedata-P Data Analysis Software (V1.9.17), respectively.

2.19. GTT and ITT

For the glucose tolerance test, mice fasted for 12 h were intraperitoneally (i.p.) injected with D-glucose (1.0 g/kg, lean mass, Sigma). For the insulin tolerance test, mice fasted for 4 h and were intraperitoneally injected with insulin (1.0 U/kg, lean mass, Beyotime). Glucose level was measured in tail blood at 0, 15, 30, 60, and 120 min after glucose or insulin injection using a glucometer (YUWELL).

2.20. Statistical analysis

All values are represented as means \pm standard error of the mean (SEM) for experiments, including the numbers of mice as indicated. All data points are biological replicates. Statistical significance was determined using a non-paired two-tailed student's t-test using the GraphPad Prism 8 software (GraphPad). Statistical significance is displayed as P < 0.05.

3. RESULTS

3.1. PHD2 expression was highly enriched in BAT, colocalized, and positively correlated with UCP1 expression

First, we detected the distribution pattern of PHDs in mice with different adipose tissues. Immunoblotting results showed that the

protein expression of PHD2 but not PHD1 and PHD3 was highly enriched in interscapular brown adipose tissue (iBAT) rather than in inguinal white adipose tissue (iWAT) and epididymal white adipose tissue (eWAT) (Figure 1A). Meanwhile, absolute quantitative PCR result demonstrated the high gene copies of PHD2 in BAT (Figure 1B). In addition, immunofluorescence staining revealed the colocalization of PHD2 with UCP1 in BAT (Figure 1C). Furthermore, the change of PHD2 expression in BAT and iWAT in response to thermogenic activation was examined. Expectedly, the protein levels of UCP1 and PHD2 in BAT (Figure 1D, E) and iWAT (Figure 1F, G) were both dramatically increased when the mice were injected with CL316243. In agreement, when treated with isoproterenol, the PHD2 and UCP1 were colocalized and both significantly increased in the differentiated brown adipocytes (Figure 1H, I). And the immunoblotting and quantitative PCR analysis also indicated the simultaneous promotion of UCP1 and PHD2 protein (Figure 1J, K) and mRNA (Figure 1L) levels. Together, these results showed that PHD2 was highly enriched in BAT, colocalized, and

positively correlated with UCP1 expression, suggesting the potential regulatory effects of PHD2 on UCP1.

3.2. Inhibition of PHD2 significantly attenuated BAT thermogenesis

To investigate the potential role of PHD2 in BAT thermogenesis, DMOG (an inhibitor of PHD) was used to construct a PHD2-inhibited model. Then, a significant reduction of dorsal interscapular surface temperature (Figure 2A–C) and rectal temperature (Figure 2D) was observed in DMOG i. p injection mice under cold exposure, but not in normal temperature (SpFig. S1a–d). Similarly, inhibition of PHD2 significantly repressed the protein (Figure 2E, F) and mRNA (Figure 2G) expression of thermogenic genes (UCP1, PGC-1 α , etc.) in cold-stimulated BAT. These data suggested that inhibition of PHD2 significantly attenuated BAT activation and thermogenesis. Although having no effect on the energy expenditure (Figure 2J, K), PHD2 inhibition resulted in a marked elevation of respiratory quotient in mice after CL316243 treatment (Figure 2H, I), which implied some degree of decrease in fatty acid

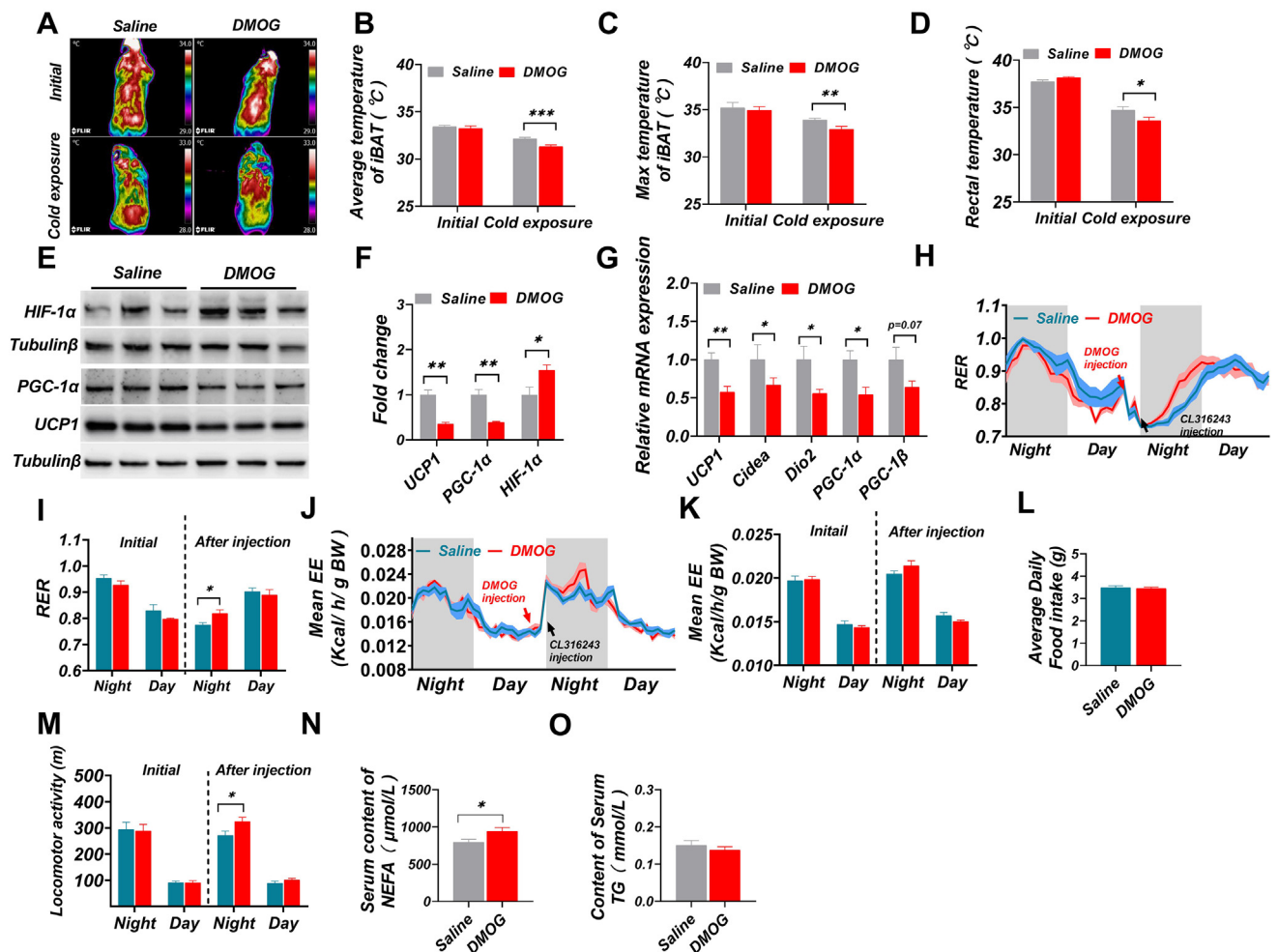


Figure 2: Inhibition of PHD2 significantly attenuated thermogenesis in BAT. A–D, Representative infrared images (A) of vehicle or DMOG injection mice were captured and displayed. Surface average temperature (B) and max temperature (C) of the interscapular BAT area, or rectal temperature (D) were determined after 8 h cold exposure. (n = 8 per group). E, RT-qPCR was performed to detect the mRNA expression level of thermogenic genes in BAT of mice injected with DMOG after 8 h cold exposure (n = 6 per group). F–G, Immunoblotting was performed (F) and the protein levels of UCP1, PGC-1 α , and HIF-1 α were quantified (G) in BAT of mice injected with DMOG after 8 h cold exposure (n = 6 per group). H–M, C57BL/6 J mice were i. p. injected with either vehicle or DMOG (40 mg per kg) and CL316243 (1 mg per kg) after a 24 h basal observation. Then the respiratory quotient (H, I), energy expenditure (J, K), daily food intake (L), and locomotor activity (M) were detected for another 24 h (n = 8 per group). N–O, Serum concentration of NEFA (N) and TG (O) were determined in mice injected with DMOG (40 mg per kg) after 8 h cold exposure (n = 8 per group). All data are presented as means \pm SEM. All data points were biological replicates. Statistical analyses were performed by the two-tailed Student's t-test between the individual groups. *P \leq 0.05, **P \leq 0.01 and ***P \leq 0.001 compared with the corresponding control group.

utilization. In line with this, the PHD2 inhibition induced an increase in non-esterified fatty acids (NEFA) content (Figure 2N) in mice serum. Together, these data demonstrated that inhibition of PHD2 attenuated BAT thermogenesis, probably due to the reduction of fatty acid utilization.

3.3. Knockdown of PHD2 significantly aggravated obesity and inhibited BAT thermogenesis of mice under HFD

Besides PHD2 inhibition, the PHD2 knockdown model by injecting PHD2-sgRNA AAV and Cas9 AAV to BAT was applied to further investigate the regulation of PHD2 on BAT thermogenesis. The specific knockdown efficiency of PHD2 in BAT was determined with PHD2 expression detection in tissues (SpFig. S2a,b). Following HFD feeding, there was no significant influence on accumulating food intake of mice between groups (SpFig. S2c). However, the body weight gain

(Figure 3A, SpFig. S2d) of PHD2-KD mice was significantly increased. Consistently, histological analyses showed that PHD2-KD mice fed with HFD exerted marked adipocyte hypertrophy in iBAT (SpFig. S2e, f). Moreover, PHD2-KD mice exhibited more severe glucose intolerance (SpFig. S2g, h), but not insulin resistance (SpFig. S2i, j) than those of control mice. These results indicated that obesity was aggravated in PHD2-KD mice under HFD feeding.

The PHD2-KD-induced exacerbation of obesity might result from impaired thermogenesis. Indeed, we observed a significant decrease in dorsal interscapular surface temperature (Figure 3B–D) and rectal temperature (Figure 3E) in PHD2-KD mice fed with HFD under cold exposure. In addition, PHD2-KD significantly suppressed the expression of the protein (Figure 3F,G) and mRNA (Figure 3H) of thermogenic genes (UCP1, PGC-1 α , and Dio2) in BAT. Finally, PHD2-KD mice elicited a significant elevation of respiratory quotient (Figure 3I,J), which

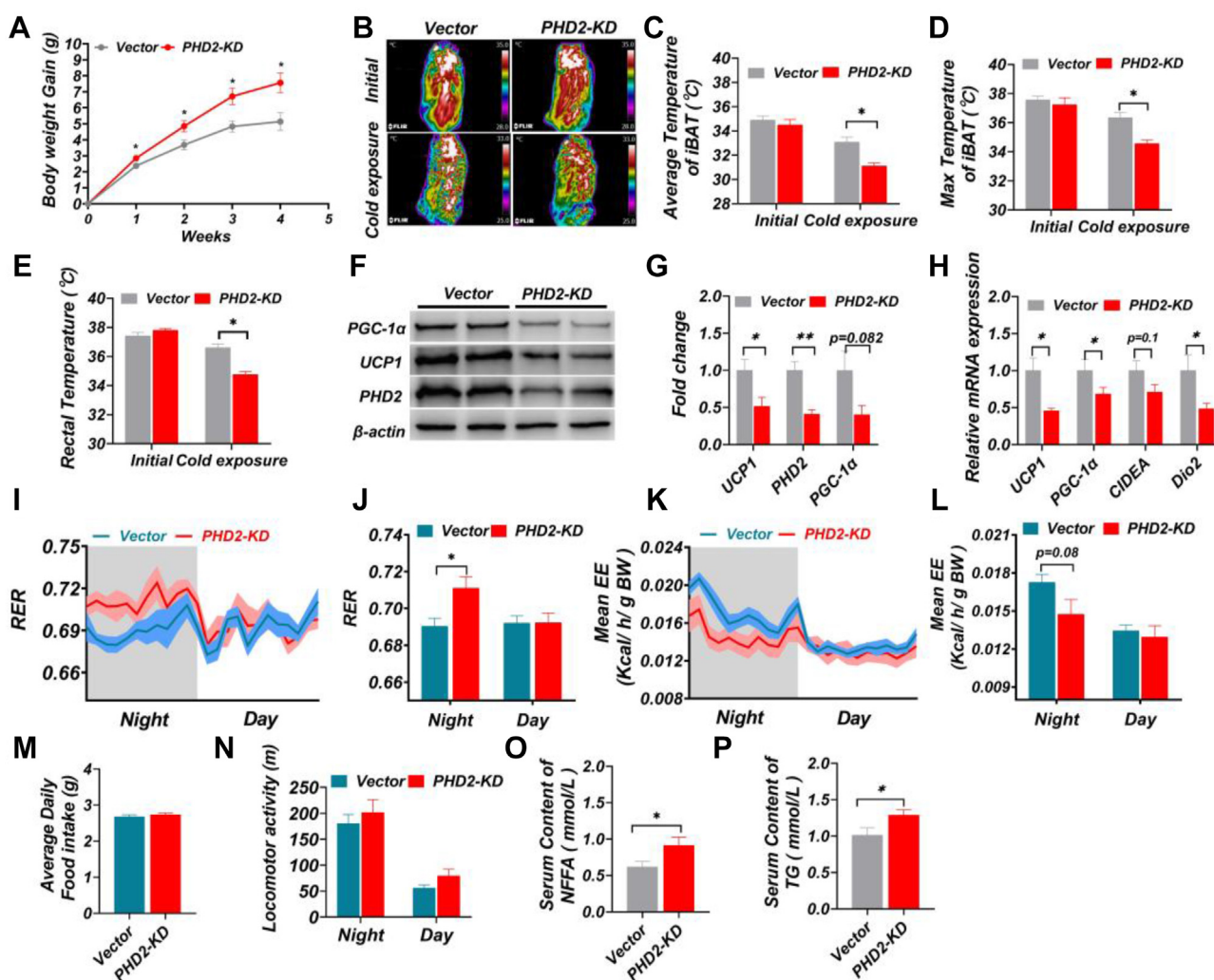


Figure 3: Knockdown of PHD2 significantly aggravated obesity and inhibits BAT thermogenesis of mice under HFD. (A) The BAT of C57BL/6 J HFD-fed mice was injected with AAV9-CAS9 virus combined with AAV9-U6-PHD2-sgRNA or AAV9-U6-scramble-sgRNA virus. Body weight gain of Vector and PHD2-KD mice were counted (n = 8 per group). (B–E) Representative infrared images (B) of Vector and PHD2-KD HFD-fed mice were captured and displayed. Surface average temperature (C) and max temperature (D) of the interscapular BAT area, or rectal temperature (E) were detected (n = 8 per group). (F–H) Immunoblotting analysis was performed (F), and protein levels of UCP1, PHD2, and PGC-1 α were quantified in BAT of Vector and PHD2-KD mice (G) (n = 4 per group). h, RT-qPCR was performed to detect the mRNA expression level of thermogenic genes in BAT of Vector and PHD2-KD mice (n = 6 per group). (I–N) Basal respiratory quotient (I, J), energy expenditure (K, L), daily food intake (M), and locomotor activity (N) were detected and quantified in Vector and PHD2-KD mice (n = 8 per group). All data are presented as means \pm SEM. (O–P) Serum concentration of TG and NEFA were determined in Vector and PHD2-KD mice (n = 8 per group). All data points are biological replicates. Statistical analyses were performed by the two-tailed Student's t-test between the individual groups. *P \leq 0.05 and **P \leq 0.01 compared with the corresponding control group.

was accompanied by an increase in serum content of triglyceride (TG) (Figure 3P) and non-esterified fatty acids (NEFA) (Figure 3O). Besides, the general energy expenditure (Figure 3K, L) of PHD2-KD mice have a decreased trend with no influence on average daily food intake and physical activity (Figure 3M, N).

Taken together, these results indicated that PHD2 played an important role in the thermogenesis of BAT in mice and PHD2-KD significantly impaired BAT thermogenesis and aggravated obesity in mice fed with HFD.

3.4. Knockdown of PHD2 suppressed brown thermogenesis of differentiated SVF independent of HIF-1 α signaling pathway

To further investigate the potential regulatory effects of PHD2 on brown adipogenesis and thermogenesis, primary stromal vascular fraction (SVF) isolated from BAT were infected with vector and PHD2-KD adenovirus and were induced to brown adipogenic differentiation. The lipid accumulation

(Figure 4A, B) and the expression of PPAR γ (Figure 4C, D) were significantly decreased by PHD2-KD, suggesting the suppression of brown adipogenesis. In addition, the protein expression of thermogenic genes such as UCP1 and PGC-1 α was significantly reduced in response to PHD2 knockdown (Figure 4C, D). Furthermore, qPCR analysis confirmed that PHD2-KD markedly decreased the mRNA levels of thermogenic genes in the differentiated brown adipocytes (Figure 4E). Together, these findings showed that knockdown of PHD2 suppressed brown adipogenesis and thermogenesis of primary SVF. In agreement, similar results were observed in the presence of PHD2 inhibition with DMOG. Expectedly, DMOG treatment significantly inhibited the brown adipogenesis (Figure 4F, G) and thermogenesis of differentiated brown adipocytes, with a remarkable reduction of protein (Figure 4H, I) and mRNA (Figure 4J) expression of adipogenic and thermogenic genes.

As the most characterized target of PHDs, the HIF-1 α signaling pathway was observed to be activated in the PHD2-KD group,

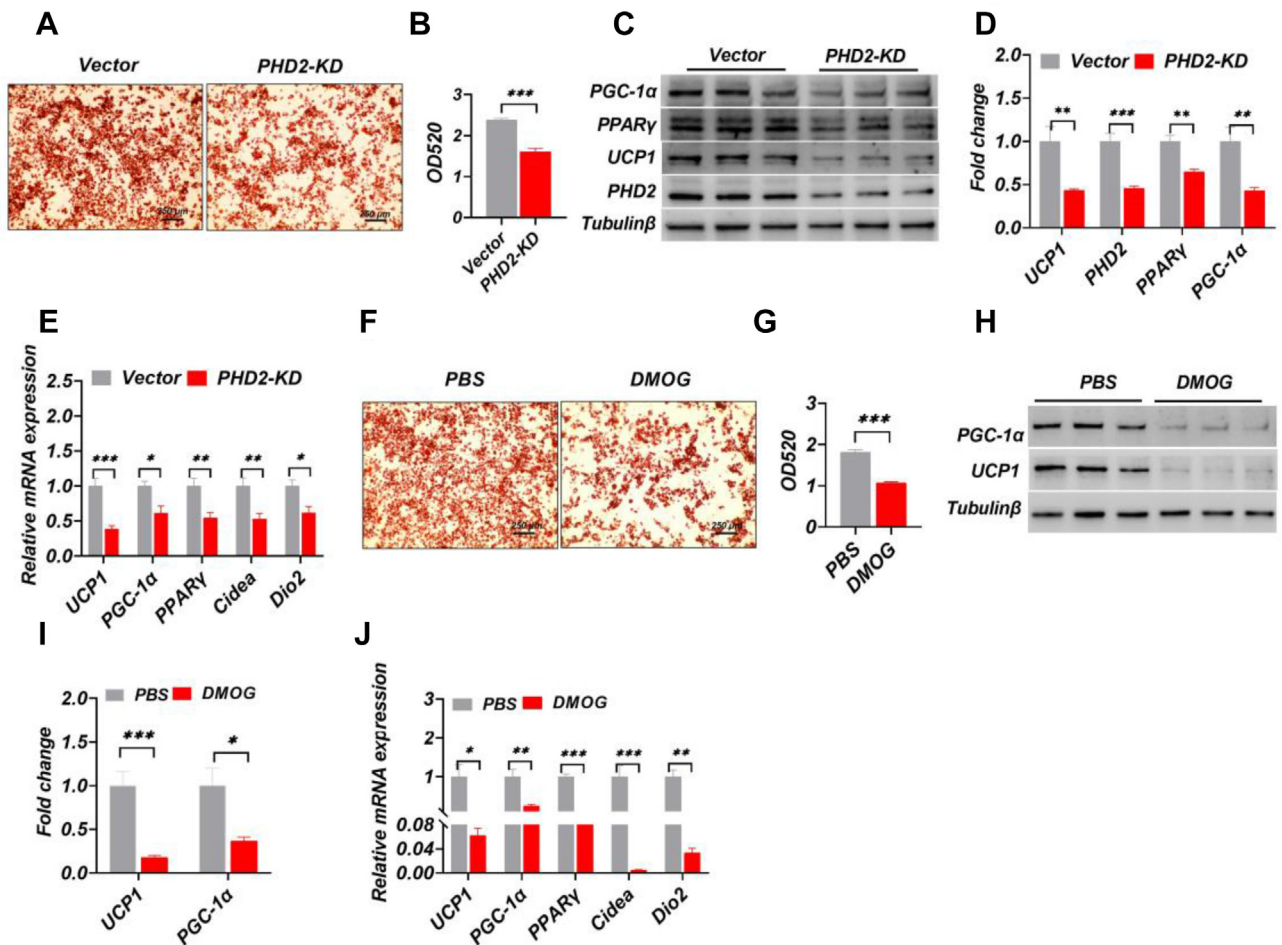


Figure 4: Knockdown of PHD2 suppressed brown adipogenesis and thermogenesis of primary stromal vascular fraction (SVF) independent of HIF-1 α . (A–B) Primary SVF isolated from BAT were transfected with vector and PHD2-KD adenovirus and differentiated to mature brown adipocytes. Oil red O staining of differentiated brown adipocytes was performed (A) and quantified (B) in Vector and PHD2-KD groups (n = 6 per group), Scale bars, 250 μ m. (C–D) Immunoblotting analysis was performed (C) and quantified (D) to detect thermogenic protein levels in Vector and PHD2-KD groups (n = 6 per group). (E) RT-qPCR was performed to detect the mRNA expression level of thermogenic genes in differentiated brown adipocytes of Vector and PHD2-KD groups (E) (n = 6 per group). (F–G) Primary SVF isolated from BAT were treated with DMOG (400 μ M) and differentiated to mature brown adipocytes. Oil red O staining of differentiated brown adipocytes was performed (F) and quantified (G) after DMOG treatment (n = 4 per group), Scale bars, 250 μ m. (H–I) Immunoblotting analysis was performed (H) and quantified (I) in differentiated brown adipocytes after DMOG treatment (n = 6 per group). (J) RT-qPCR was performed to detect mRNA expression of thermogenic and adipogenic genes in differentiated brown adipocytes after DMOG treatment (J) (n = 6 per group). All data are presented as means \pm SEM. All data points are biological replicates. Statistical analyses were performed by the two-tailed Student's t-test between the individual groups. *P \leq 0.05, **P \leq 0.01 and ***P \leq 0.001 compared with the corresponding control group. (For interpretation of the references to color in this figure legend, the reader is referred to the Web version of this article.)

indicated by the increased lactate content and decreased pH value in the culture medium (SpFig. S3a–c). In addition, the PHD2-KD-induced alterations of pH value (SpFig. S3d, e) and (SpFig. S3f) lactate content were reversed by HIF-1 α interference. And the impaired brown adipogenesis caused by PHD2-KD was partly rescued (SpFig. S3g, h). However, the decreased protein (SpFig. S3i, j) and mRNA (SpFig. S3k) expression of thermogenic genes by PHD2-KD had no significant response to HIF-1 α interference. These data suggested that the knockdown of PHD2 inhibited brown thermogenesis of the differentiated SVF independent of HIF-1 α signaling.

3.5. Mitochondrial PHD2 bound to UCP1 and regulated the hydroxylation level of UCP1

Excluding the involvement of HIF-1 α signaling and considering the colocalization of PHD2 and UCP1, we thus investigated the possible direct interaction between PHD2 and UCP1. We found that PHD2 and UCP1 were both enriched in the cytoplasm but not nucleus (Figure 5A). Given that mitochondria are the fundamental organelles for thermogenesis, we further examined the PHD2 expression in mitochondrial

and observed the clear existence of PHD2 in mitochondria (Figure 5B), confirming the colocalization with UCP1. In addition, the mitochondrial PHD2 was significantly elevated in response to isoproterenol treatment (Figure 5C), suggesting that mitochondrial PHD2 was closely related to thermogenic activation. Furthermore, the results of the co-IP analysis revealed the direct binding of PHD2 with UCP1 but not with PGC-1 α or Prdm16 in BAT (Figure 5D). Moreover, the binding level between PHD2 and UCP1 was enhanced with the BAT activation by CL316243 treatment (Figure 5D).

Given the hydroxylation function of PHDs, we examined the overall hydroxylation level of proteins in PHD2-KD adipocytes. The results showed that hydroxylation modification was detected in both total cell protein (Figure 5E, left panel) and cytoplasmic protein (Figure 5E, middle panel). More interestingly, abundant hydroxylation modification also existed in mitochondrial proteins (Figure 5E, right panel). With PHD2-KD, the hydroxylation modification of the specific proteins was significantly reduced, especially around 35 kDa (UCP1 molecular weight is around 33 kDa) (Figure 5E, right panel). Moreover, we found that the hydroxylation level of UCP1 in the differentiated brown adipocytes was

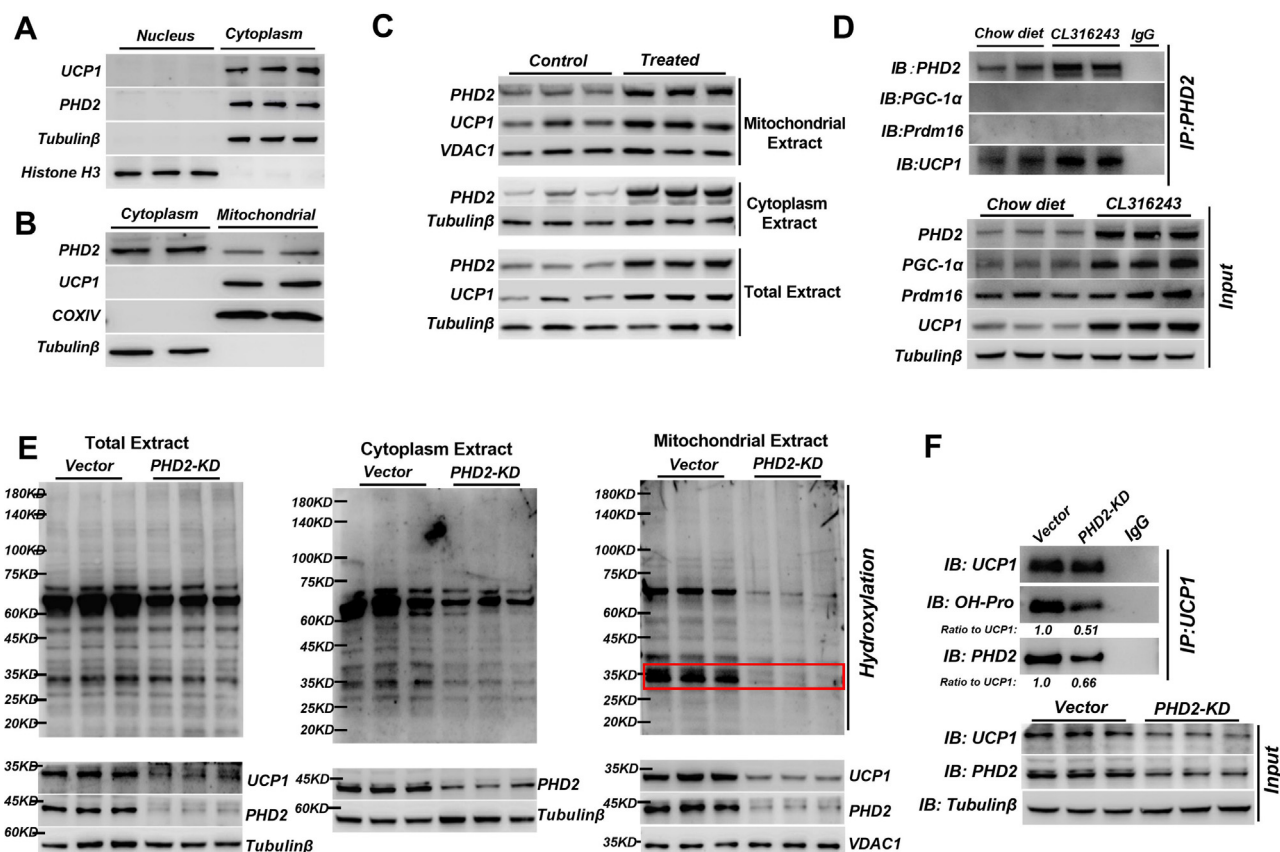


Figure 5: Mitochondrial PHD2 bound to UCP1 and regulated the hydroxylation level of UCP1. (A–B) Immunoblotting analysis was performed to detect the distribution and expression of PHD2 in the cytoplasm, nucleus (A), and mitochondrial (B) protein in BAT ($n = 3$ per group). (C) The differentiated brown adipocytes were treated with vehicle or isoproterenol (10 μ M) for 24 h. Immunoblotting analysis was performed (C) to detect the protein level of PHD2 expression in different cell components ($n = 6$ per group). (D) C57BL/6 J mice were i.p. injected with either vehicle or CL316243 (1 mg per kg) every other day for a week. Co-IP assay was performed (D) to detect potential binding targets of PHD2 in BAT. (E) Primary SVF isolated from BAT were transfected with vector and PHD2-KD adenovirus. Immunoblotting analysis was performed (E) to determine the effects of PHD2-KD on the hydroxylation modification in total (left panel), cytoplasm (middle panel), and mitochondrial (right panel) proteins of the differentiated brown adipocytes ($n = 3$ per group). The red box indicated the band around 35 kDa. (F) Co-IP assay was performed (F) to determine the effects of PHD2-KD on the hydroxylation level of UCP1 and the binding level of UCP1 with PHD2 in the differentiated brown adipocytes.

significantly reduced in response to PHD2-KD (Figure 5F). Collectively, these results indicated that the mitochondrial PHD2 could bind to UCP1 and regulate the hydroxylation level of UCP1.

3.6. PHD2 promoted the expression and stability of UCP1 protein by hydroxylating UCP1 proline residues in HEK 293T cells

Further, the HEK 293T cells transfected with various plasmids were used to explore the specific mechanism of UCP1 hydroxylation by PHD2. Based on the similar transfection efficiency of fluorescent plasmids among groups (SpFig. S4a), we found that the expression of UCP1 increased significantly in response to PHD2 overexpression (SpFig. S4b, c). In addition, the results of co-IP revealed that the binding level between PHD2 and UCP1, as well as the hydroxylation modification level of UCP1 were markedly enhanced by PHD2 overexpression (Figure 6A, B, SpFig. S4f). Furthermore, to determine the

role of PHD2 on UCP1 protein hydroxylation modification, the cell-free simulated hydroxylation modification assay was carried out as indicated (Figure 6C). The results showed that under a similar amount of input UCP1 protein, the UCP1 hydroxylation level indicated as a ratio to UCP1 was significantly elevated by PHD2 overexpression (Figure 6D). As hydroxylation has been reported to be closely related with the protein stability, we further evaluated the protein stability of UCP1. The results indicated that the UCP1 protein level was significantly decreased by cycloheximide (CHX, a protein synthesis inhibitor). However, in the presence of PHD2 overexpression, the CHX no longer induced the reduction of the UCP1 protein level (Figure 6E), suggesting that the UCP1 stability was enhanced by PHD2 overexpression. Together, it could be concluded that PHD2 overexpression enhanced the hydroxylation of UCP1 and promoted the expression and stability of the UCP1 protein.

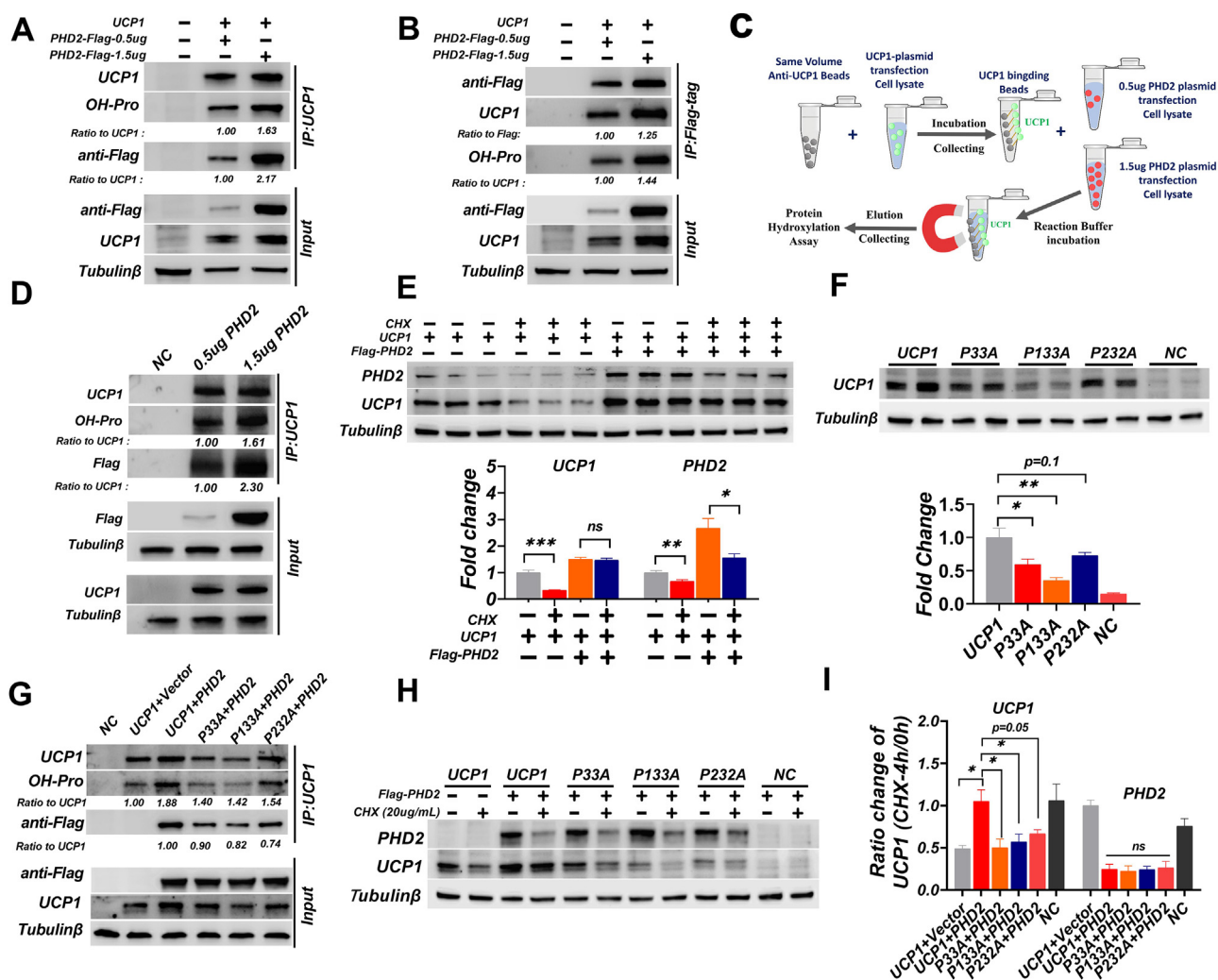


Figure 6: PHD2 promotes the expression and stability of UCP1 protein by hydroxylating the specific proline residues of UCP1 in HEK 293T cells. (A–B) HEK 293T cells were transfected with UCP1 and different dose Flag-PHD2 plasmids (0.5 µg/1.5 µg). The hydroxylation level of UCP1 protein and its binding level with PHD2 in cells of PHD2-OE were detected by Co-IP assay. (C–D) Schematic diagram of cell-free simulated UCP1 hydroxylation test (C). The hydroxylation of UCP1 protein was determined (D) in the cell-free system as indicated in C. (E) HEK 293T cells were transfected with vector or Flag-PHD2 plasmid and treated with cycloheximide (CHX, 20 µg/ml) for 8 h. Immunoblotting analysis was performed and the stability of UCP1 protein was detected and analyzed (E) (n = 6 per group). (F–I) HEK 293T cells were transfected with various proline mutation plasmids targeting UCP1. Immunoblotting analysis was performed and the UCP1 protein level was quantified (F) (n = 4 per group). The hydroxylation level of UCP1 protein and its binding level with PHD2 was determined by Co-IP assay (G). Immunoblotting analysis was performed (H) and UCP1 stability was quantified (I) under CHX treatment (n = 3 per group). All data are presented as means ± SEM. All data points are biological replicates. Statistical analyses were performed by the two-tailed Student's t-test between the individual groups. *P ≤ 0.05, **P ≤ 0.01 and ***P ≤ 0.001 compared with the corresponding control group.

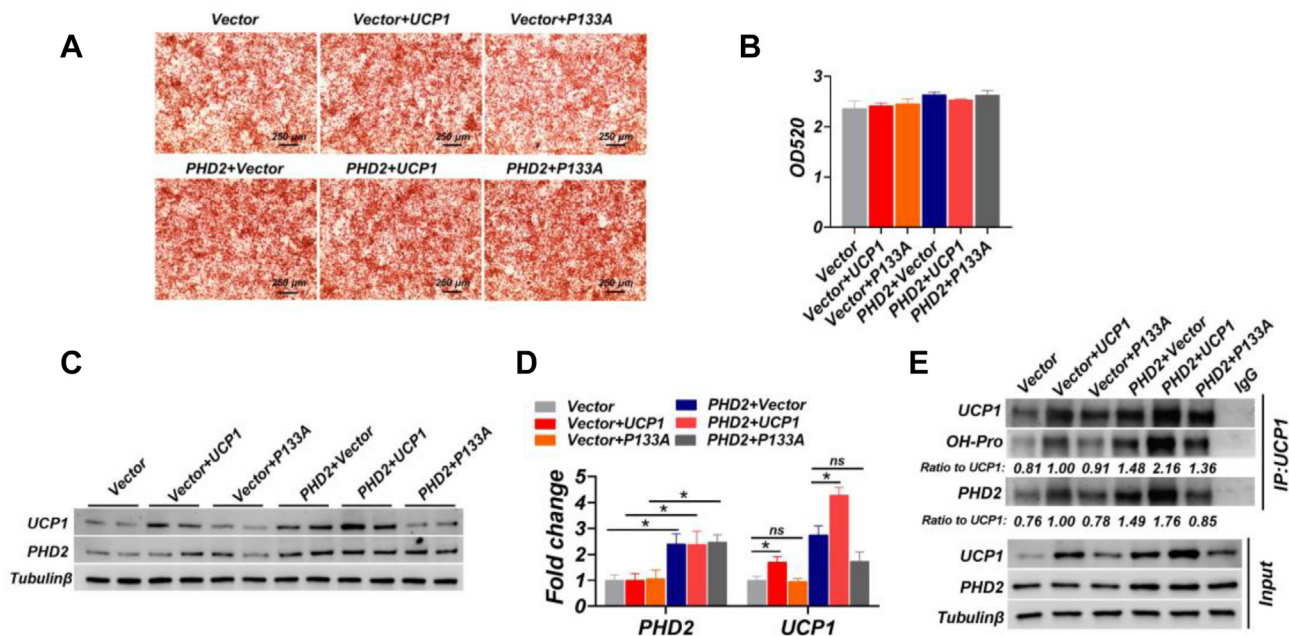


Figure 7: PHD2 promoted UCP1 expression in differentiated SVF isolated from BAT by hydroxylating UCP1-133 proline residues. (A–E) Primary SVF isolated from BAT were transfected with UCP1, PHD2, and P133A UCP1 lentivirus and differentiated to mature brown adipocytes. Oil red O staining was displayed (A) and quantified (B) with transfected brown adipocytes (n = 4 per group). Immunoblotting analysis was performed (C) and protein levels of UCP1 and PHD2 were quantified (D) in vitro (n = 4 per group). (E) Co-IP assay was performed to determine the hydroxylation level of UCP1 protein and its binding level with PHD2 after lentivirus transfection. All data are presented as means ± SEM. All data points are biological replicates. Statistical analyses were performed by the two-tailed Student's t-test between the individual groups. *P ≤ 0.05 compared with the corresponding control group.

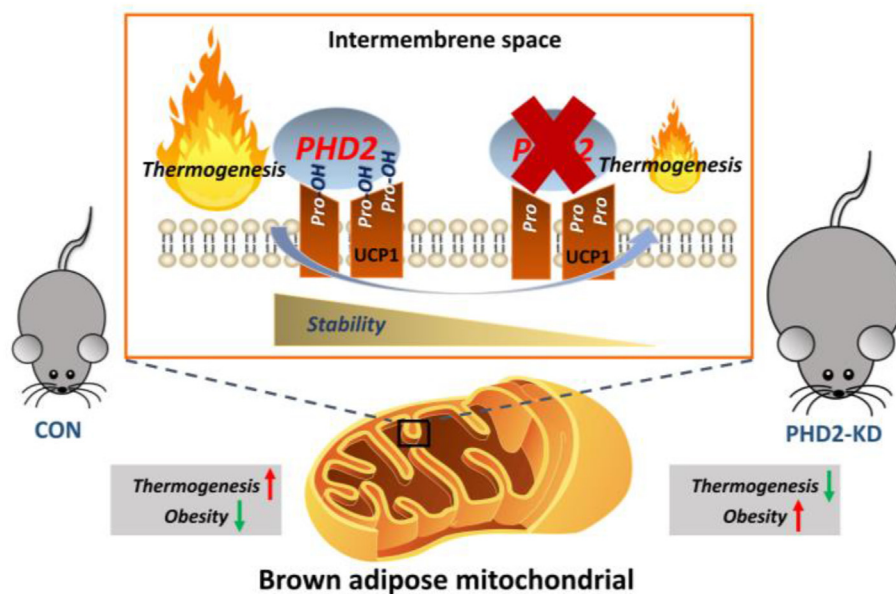


Figure 8: PHD2 promoted brown adipose thermogenesis by enhancing the hydroxylation and stability of UCP1. The schematic working model illustrated that PHD2 promoted BAT thermogenesis by enhancing the hydroxylation-dependent expression and stability of the UCP1 protein. In contrast, inhibition or knockdown of PHD2, as well as mutation of proline residues in UCP1, significantly inhibited the expression and stability of UCP1, and thus suppressed BAT thermogenesis. Furthermore, PHD2 knockdown-induced reduction of UCP1 aggravated obesity of mice under HFD. (For interpretation of the references to color in this figure legend, the reader is referred to the Web version of this article.)

The next issue to be confirmed is which proline residues are involved in UCP1 hydroxylation modification by PHD2. It has been reported that a highly conserved amino acid sequence [P] X [D/E] X X [K/R] containing proline is crucial for the UCP1 protein structure and function [43–45].

To this end, we analyzed the amino acid sequence of UCP1 in different species and found that the Pro33, Pro133, and Pro232 were coincident with the conserved sequence. More importantly, the potential hydroxylated proline residues in BAT of mice under cold exposure were

determined by mass spectrometer analysis. The results confirmed the existence of the expected hydroxylated mass shift of Pro33, Pro133, and Pro232 in peptides (SpFig. S5b–e). Therefore, the mutation (Pro to Ala) plasmids targeting the Pro33, Pro133, and Pro232, named P33A, P133A, and P232A respectively, were constructed to transfect HEK 293T cells (SpFig. S4d, e). Based on the similar transfection efficiency of plasmids (SpFig. S4g), we found that, compared with the wild-type UCP1 plasmid, the mutation plasmids significantly inhibited the protein level of UCP1 (Figure 6F) and reduced the PHD2-elevated hydroxylation level (Figure 6G). Besides, the increased UCP1 stability induced by PHD2 overexpression was reversed by the transfection of UCP1 mutant plasmids (Figure 6H,I).

3.7. PHD2 overexpression promotes UCP1 expression in differentiated SVF isolated from BAT by hydroxylating UCP1-133 proline residues

In light of UCP1 P133A elicited the most effective inhibition on UCP1 hydroxylation in 293T cells. Further, the role of specific proline residue 133 in UCP1 was confirmed in differentiated brown adipocytes by transfecting P133A lentivirus to primary SVF. The fluorescence pictures and oil red O staining revealed similar transfection efficiency and adipogenesis level among groups (SpFig. S4h, Figure 7A, B). Expectedly, the protein level of UCP1 was significantly increased by PHD2 overexpression, while P133A transfection reversed the effect (Figure 7C, D). Furthermore, the hydroxylation assay showed that P133A attenuated the PHD2-induced hydroxylation of UCP1 in brown differential adipocytes (Figure 7E). Taken together, these data demonstrated that PHD2 promoted the expression and stability of UCP1 protein by hydroxylating the specific proline residues of UCP1.

4. DISCUSSION

In this study, we demonstrated that PHD2 promoted brown adipose thermogenesis by enhancing the hydroxylation of UCP1. PHD2 belongs to a 2-oxoglutarate-dependent oxygenase superfamily and it is widely exists in the body [17], especially in adipose tissue [46]. In our research, PHD2 was also detected as more abundant than PHD1 and PHD3 in BAT of mice which were similar to the results of Heidenreich [47]. Recently, some studies have revealed that PHD2 was highly colocalized in mitochondria. For instance, Khan et al. and Barth et al. discovered mitochondrial and peroxisomal localization of PHD2 in their studies [48,49]. Angelini et al. demonstrated that PHD2 could bind to CPT1B which is located in the mitochondrial membrane [25]. Moreover, according to mass spectrometry data shared by Meyer et al. PHD2, but not PHD1 and PHD3, was found to exist in mitochondrial protein [50]. By detecting cytoplasmic protein and mitochondrial protein, we observed that PHD2 exists in both components. What is more, PHD2, but not PHD1 or PHD3, showed an evident correlation with UCP1, suggesting PHD2 may be closely related to the mitochondrial thermogenesis process in BAT. Overall, our findings indicated that PHD2 expression was highly enriched in BAT, colocalized, and positively correlated with UCP1 expression.

UCP1 is an important executor of mitochondrial thermogenesis. Our study further investigated the effect of PHD2 on BAT thermogenesis in vitro and in vivo. It has been reported that DMOG (pan inhibitor of PHDs) and hypoxia exposure (known to inhibit PHDs) can significantly inhibit adipocytes lipolysis, thermogenesis, and cause intolerance to cold stimulation in mice [51–54]. Consistent with the research, we showed the impaired thermogenic capacity of BAT and primary brown adipocytes by treating with DMOG. It has been reported that UCP1 activation participates in the fat deposition of mice and humans. UCP1

activation enhances body energy consumption and reduces fat deposition in mice and humans [55,56]. Meanwhile, inhibition of UCP1 aggravates obesity [57–60]. In our study, we found knockdown of PHD2 in BAT and primary brown adipocytes also exhibited the dysfunction of thermogenesis, with increasing body and adipose weights in HFD mice. Although, in some cases, several researches showed UCP1–KO had no effect on body weight and fat deposition in mice [61–63], which might due to the difference in UCP1 activation status under different dietary types or ambient temperatures.

Recently, PHD2 was found to promote mitochondrial fatty acids β -oxidation [25,64], and systemic adipose-selective PHD2 deletion significantly repressed β -adrenergic receptor-induced lipolysis and NEFA release which is important to BAT adaptive activation [28]. Indeed, we observed an elevation in the respiratory quotient and serum NEFA content of mice which showed the disorder of fatty acids utilization. It is interesting to note that the temperature maintenance disorder and respiratory entropy increase of PHD2-KD mice were significant only after cold stimulation or during the feeding period at night in our observation which is reminiscent of those UCP1-knockout mice [57,65]. Therefore, this further indicated that PHD2 plays a more important role in the activation of BAT. The total energy expenditure (TEE) of the body is contributed by several parts including resting metabolic rate (RMR), activity energy expenditure (AEE), and energy due to the thermogenic effect [66,67]. The contribution of differential activity levels to energy expenditure of mice was determined in several published studies [68–70]. In Figure 2, we did not observe a significant decrease in TEE after DMOG treatment. However, we found that the locomotor activity of mice was significantly increased, which reflected that there exists more AEE. This could be the reason why the TEE of mice injected with DMOG did not change. In addition, DMOG is a pan-inhibitor of PHDs and previous study has found that PHD3 knockout in skeletal muscle promote muscular energy expenditure and exercise capacity, which may also lead to a compensatory effects on TEE [71]. The specific reason why intraperitoneal injection of DMOG increased the locomotor activity of mice is unclear. But, it was reported that knocking out P4H-tm, a member of PHDs, could significantly increase the locomotor activity and social behavior of mice which may provide an explanation [72]. Overall, our research showed that the inhibition and knockdown of PHD2 attenuated the thermogenesis process of BAT in vivo and in vitro experiments.

The HIF signal pathway is the main substrate for PHD2 to perform its regulatory role. At present, in reports signed by Michailidou and Matsuura, adipose-selective PHD2 knockout in whole body elevated the BAT function and energy consumption enhancement of mice through activation of the HIF α signal pathway which is distinct from our research [73,74]. Actually, the effects of HIF α on adipose are complex and miscellaneous. For instance, it has been reported that HIF α is a molecular brake to inhibit the thermogenesis process [53,75,76] and fatty acids β -oxidation [77,78]. Therefore, the complexity of HIF α regulated function may be the reason for the discrepancy between our results. Besides, systemic adipose complete deletion of PHD2 resulted in a greater enhancement of glucose consumption and metabolism in the whole body (white adipose and skeletal muscle) and may cover the effect of PHD2 on a single BAT. Additionally, the functional differences of BAT under the different ambient temperatures, knock-down method, and efficiency may also contribute to the divergence.

In our study, the role of HIF-1 α (The major regulatory substrates of PHD2) [68] in PHD2-regulated thermogenesis was explored. However, HIF-1 α interference didn't alter the thermogenesis suppression of brown adipocytes with PHD2-KD but significantly reversed the

lipogenesis dysfunction. Therefore, there may exist distinct regulated ways from HIF-1 α in PHD2-mediated thermogenesis which need further verification. Given these observations, we supposed whether exist other substrates regulated by PHD2 to participate in thermogenesis and carried out the next research.

Hydroxylation is the main mode of PHD2 to exert its regulatory function. Recently, many reports on the HIF-independent regulation of PHD2 like AKT [20], PDE4D [64], CPT1B [25], NDRG3 [79], and EGFR [80] have been found which broaden the range of PHD2-regulated hydroxylation modification. Our study found that PHD2 mediated overall intracellular protein hydroxylation level, especially in mitochondrial protein. In this regard, we tested the binding level between PHD2 and thermogenic protein. It is of interest that UCP1, but not PGC-1 α and Prdm16 (the important thermogenic regulatory factors), is bound to PHD2 and then promotes the binding level with thermogenesis activation. It has been reported that UCP1 contains a variety of post-translation modifications such as sulfenylation [12], succinylation [13], phosphorylation [14], and ubiquitination [15] which are involved in its protein activity and expression. Therefore, we further confirmed whether hydroxylation exists on UCP1. Obviously, in primary brown adipocytes and 293T cells, the PHD2 expression level positively regulated the protein expression and hydroxylation of UCP1 simultaneously. Therefore, based on the observations, we concluded PHD2 played an important role in promoting the expression and hydroxylation level of UCP1 protein.

[P] X [D/E] X X [K/R] is the sequence found at the kinks of L-sharped- α -helices [45,81], which is highly conserved in UCP1 of various species by our comparison. It was reported that α -helix participates in the formation of the salt bridge structure [82] and is essential for UCP1 stability by binding UCP1 to the mitochondrial inner membrane lipids [44]. As three proline residues (Pro33, Pro133, Pro232) were analyzed in our research located at the beginning of the helices and coincident to [P] X [D/E] X X [K/R] motif in UCP1. In particular, mass spectrometry analysis also confirmed the hydroxylated proline residues. Therefore, we selected the three sites for further research. Several previous studies have shown that hydroxylation modification exhibited a dual character in protein stability regulation [20,21,26,80]. Herein, we found PHD2 significantly enhanced UCP1 stability markedly under CHX treatment in 293T cells which is consistent with the previous phenotype. While P33A, P133A, and P232A mutant transfection all reversed the hydroxylation level and protein stability of UCP1 to a certain extent. Therefore, we speculated that the hydroxylation of UCP1 may occur at multiple sites and the mechanism of these sites' crosstalk between UCP1 hydroxylation and stability remains to be determined. Finally, another interesting point is PHD2 knockdown inhibited the mRNA expression of UCP1 and other thermogenic genes. The specific regulation mode is unclear. But it was reported that UCP1 protein participates in the regulation of the respiratory chain and AMPK activation [6,65,83,84]. In this study, knockdown of PHD2 also significantly reduced the AMPK protein expression level (data not shown). Therefore, whether the impairment of UCP1 protein function will affect the expression of thermogenic genes in coordination with the dysfunction of AMPK or the mitochondrial respiratory chain needs to be further confirmed.

In summary, in our research, PHD2-dependent regulation exerted a crucial role in the control of UCP1 level and thermogenesis in brown adipocytes. The coincident effects were seen in both knockdown and inhibition of PHD2 in vivo or in vitro models. Mechanistically, PHD2 bound to UCP1 and mediated its protein stability through a hydroxylation modification mode while mutation of the specific prolines in UCP1

eliminated the effects of PHD2. In addition, the PHD2-regulated protein stability of UCP1 affected the utilization of intracellular fatty acids and lipid deposition (Figure 8). Overall, this study showed that PHD2 promoted brown adipose thermogenesis by enhancing hydroxylation of UCP1, providing the new regulatory target for UCP1 activity and BAT thermogenesis.

AUTHOR CONTRIBUTIONS

Songbo Wang, Qingyan Jiang, and Fan Li designed the project and experiments. Fan Li, Fenglin Zhang, Xin Yi, Lulu Quan, and Xiaohua Yang performed the experiments. Fan Li, Cong Yin, Zewei Ma, Ruifan Wu, Weijie Zhao, and Mingfa Lin collected, analyzed, and interpreted researched data. Xiaotong Zhu and Ping Gao contributed to experimental methods and helpful discussion. Qingyan Jiang, Gang Shu, Fan Li, Lina Wang, Qianyun Xi, Yongliang Zhang, and Lin Zhang reviewed the manuscript. Fan Li wrote the manuscript. Abdelaziz Hussein, Limin Lang, and Canjun Zhu improved the syntax of the manuscript. Songbo Wang edited the manuscript. Songbo Wang and Qingyan Jiang supervised the work. All authors approved the final manuscript.

FUNDING

This work was supported by the National Natural Science Foundation of China (32172682, 31972636, 31790411) and Guangdong Basic and Applied Basic Research Foundation (2020A1515010261).

DECLARATION OF COMPETING INTEREST

The authors declare that they have no known competing financial interests or personal relationships that could have appeared to influence the work reported in this paper.

DATA AVAILABILITY

Data will be made available on request.

APPENDIX A. SUPPLEMENTARY DATA

Supplementary data to this article can be found online at <https://doi.org/10.1016/j.molmet.2023.101747>.

REFERENCES

- [1] Marlatt KL, Ravussin E. Brown adipose tissue: an update on recent findings. *Curr Obes Rep* 2017;6:389–96.
- [2] Cypess AM, Lehman S, Williams G, Tal I, Rodman D, Goldfine AB, et al. Identification and importance of brown adipose tissue in adult humans. *N Engl J Med* 2009;360:1509–17.
- [3] Cypess AM, Weiner LS, Roberts-Toler C, Franquet Elía E, Kessler SH, Kahn PA, et al. Activation of human brown adipose tissue by a β 3-adrenergic receptor agonist. *Cell Metabol* 2015;21:33–8.
- [4] Chouchani ET, Kazak L, Spiegelman BM. New advances in adaptive thermogenesis: UCP1 and beyond. *Cell Metabol* 2019;29:27–37.
- [5] Li L, Li B, Li M, Speakman JR. Switching on the furnace: regulation of heat production in brown adipose tissue. *Mol Aspect Med* 2019;68:60–73.
- [6] Kazak L, Chouchani ET, Stavrovskaya IG, Lu GZ, Jedrychowski MP, Egan DF, et al. UCP1 deficiency causes brown fat respiratory chain depletion and sensitizes mitochondria to calcium overload-induced dysfunction. *Proc Natl Acad Sci U S A* 2017;114:7981–6.

- [7] Meyer CW, Willershäuser M, Jastroch M, Rourke BC, Fromme T, Oelkrug R, et al. Adaptive thermogenesis and thermal conductance in wild-type and UCP1-KO mice. *Am J Physiol Regul Integr Comp Physiol* 2010;299:R1396–406.
- [8] Hankir MK, Kranz M, Keipert S, Weiner J, Andreassen SG, Kern M, et al. Dissociation between Brown adipose tissue (18)F-FDG uptake and thermogenesis in uncoupling protein 1-deficient mice. *J Nucl Med* 2017;58:1100–3.
- [9] Stram AR, Payne RM. Post-translational modifications in mitochondria: protein signaling in the powerhouse. *Cell Mol Life Sci* 2016;73:4063–73.
- [10] Vu LD, Gevaert K, De Smet I. Protein Language: post-translational modifications talking to each other. *Trends Plant Sci* 2018;23:1068–80.
- [11] Walsh CT, Garneau-Tsodikova S, Gatto Jr GJ. Protein posttranslational modifications: the chemistry of proteome diversifications. *Angew Chem* 2005;44:7342–72.
- [12] Chouchani ET, Kazak L, Jedrychowski MP, Lu GZ, Erickson BK, Szpyt J, et al. Mitochondrial ROS regulate thermogenic energy expenditure and sulfonylation of UCP1. *Nature* 2016;532:112–6.
- [13] Wang G, Meyer JG, Cai W, Softic S, Li ME, Verdin E, et al. Regulation of UCP1 and mitochondrial metabolism in Brown adipose tissue by reversible succinylation. *Mol Cell* 2019;74:844–857.e847.
- [14] Carroll AM, Porter RK, Morrice NA. Identification of serine phosphorylation in mitochondrial uncoupling protein 1. *Biochim Biophys Acta* 2008;1777:1060–5.
- [15] Clarke KJ, Adams AE, Manzke LH, Pearson TW, Borchers CH, Porter RK. A role for ubiquitylation and the cytosolic proteasome in turnover of mitochondrial uncoupling protein 1 (UCP1). *Biochim Biophys Acta* 2012;1817:1759–67.
- [16] Semenza GL. HIF-1, O(2), and the 3 PHDs: how animal cells signal hypoxia to the nucleus. *Cell* 2001;107:1–3.
- [17] Fong GH, Takeda K. Role and regulation of prolyl hydroxylase domain proteins. *Cell Death Differ* 2008;15:635–41.
- [18] Place TL, Domann FE. Prolyl-hydroxylase 3: evolving roles for an ancient signaling protein. *Hypoxia* 2013;2013:13–7.
- [19] Lee JW, Bae SH, Jeong JW, Kim SH, Kim KW. Hypoxia-inducible factor (HIF-1)alpha: its protein stability and biological functions. *Exp Mol Med* 2004;36:1–12.
- [20] Guo J, Chakraborty AA, Liu P, Gan W, Zheng X, Inuzuka H, et al. pVHL suppresses kinase activity of Akt in a proline-hydroxylation-dependent manner. *Science* 2016;353:929–32.
- [21] Zheng X, Zhai B, Koivunen P, Shin SJ, Lu G, Liu J, et al. Prolyl hydroxylation by EglN2 destabilizes FOXO3a by blocking its interaction with the USP9x deubiquitinase. *Genes Dev* 2014;28:1429–44.
- [22] Rodriguez J, Herrero A, Li S, Rauch N, Quintanilla A, Wynne K, et al. PHD3 regulates p53 protein stability by hydroxylating proline 359. *Cell Rep* 2018;24:1316–29.
- [23] Luo W, Hu H, Chang R, Zhong J, Knabel M, O’Meally R, et al. Pyruvate kinase M2 is a PHD3-stimulated coactivator for hypoxia-inducible factor 1. *Cell* 2011;145:732–44.
- [24] German NJ, Yoon H, Yusuf RZ, Murphy JP, Finley LW, Laurent G, et al. PHD3 loss in cancer enables metabolic reliance on fatty acid oxidation via deactivation of ACC2. *Mol Cell* 2016;63:1006–20.
- [25] Angelini A, Saha PK, Jain A, Jung SY, Mynatt RL, Pi X, et al. PHDs/CPT1B/VDAC1 axis regulates long-chain fatty acid oxidation in cardiomyocytes. *Cell Rep* 2021;37:109767.
- [26] Li S, Li W, Yuan J, Bullova P, Wu J, Zhang X, et al. Impaired oxygen-sensitive regulation of mitochondrial biogenesis within the von Hippel-Lindau syndrome. *Nat Metab* 2022;4:739–58.
- [27] Kim J, Kwak HJ, Cha JY, Jeong YS, Rhee SD, Cheon HG. The role of prolyl hydroxylase domain protein (PHD) during rosiglitazone-induced adipocyte differentiation. *J Biol Chem* 2014;289:2755–64.
- [28] Michailidou Z, Morton NM, Moreno Navarrete JM, West CC, Stewart KJ, Fernández-Real JM, et al. Adipocyte pseudohypoxia suppresses lipolysis and facilitates benign adipose tissue expansion. *Diabetes* 2015;64:733–45.
- [29] Yin C, Ma Z, Li F, Duan C, Yuan Y, Zhu C, et al. Hypoxanthine induces muscular ATP depletion and fatigue via UCP2. *Front Physiol* 2021;12:647743.
- [30] Duan C, Yin C, Ma Z, Li F, Zhang F, Yang Q, et al. Trans 10, cis 12, but not cis 9, trans 11 conjugated linoleic acid isomer enhances exercise endurance by increasing oxidative skeletal muscle fiber type via toll-like receptor 4 signaling in mice. *J Agric Food Chem* 2021;69:15636–48.
- [31] Wu R, Cao S, Li F, Feng S, Shu G, Wang L, et al. RNA-binding protein YBX1 promotes brown adipogenesis and thermogenesis via PINK1/PRKN-mediated mitophagy. *FASEB J* 2022;36:e22219.
- [32] Yau WW, Singh BK, Lesmana R, Zhou J, Sinha RA, Wong KA, et al. Thyroid hormone (T(3)) stimulates brown adipose tissue activation via mitochondrial biogenesis and MTOR-mediated mitophagy. *Autophagy* 2019;15:131–50.
- [33] Wu R, Feng S, Li F, Shu G, Wang L, Gao P, et al. Transcriptional and post-transcriptional control of autophagy and adipogenesis by YBX1. *Cell Death Dis* 2023;14:29.
- [34] Zhu C, Xu P, He Y, Yuan Y, Wang T, Cai X, et al. Heparin increases food intake through AgRP neurons. *Cell Rep* 2017;20:2455–67.
- [35] Yuan Y, Xu P, Jiang Q, Cai X, Wang T, Peng W, et al. Exercise-induced α -ketoglutaric acid stimulates muscle hypertrophy and fat loss through OXGR1-dependent adrenal activation. *EMBO J* 2020;39:e103304.
- [36] Dieckmann S, Maurer S, Kleigrew K, Klingenspor M. Spatial recruitment of cardiolipins in inguinal white adipose tissue after cold stimulation is independent of UCP1. *Eur J Lipid Sci Technol* 2022;124:2100090.
- [37] Chini V, Foka A, Dimitracopoulos G, Spiliopoulou I. Absolute and relative real-time PCR in the quantification of *tst* gene expression among methicillin-resistant *Staphylococcus aureus*: evaluation by two mathematical models. *Lett Appl Microbiol* 2007;45:479–84.
- [38] Li Y, Chen L, Zhao W, Sun L, Zhang R, Zhu S, et al. Food reward depends on TLR4 activation in dopaminergic neurons. *Pharmacol Res* 2021;169:105659.
- [39] Luo W, Lin B, Wang Y, Zhong J, O’Meally R, Cole RN, et al. PHD3-mediated prolyl hydroxylation of nonmuscle actin impairs polymerization and cell motility. *Mol Biol Cell* 2014;25:2788–96.
- [40] Wu B, Song Q, Li W, Xie Y, Luo S, Tian Q, et al. Characterization and functional study of a chimera galectin from yellow drum *Nibea albiflora*. *Int J Biol Macromol* 2021;187:361–72.
- [41] Xie Z, Yu W, Zheng G, Li J, Cen S, Ye G, et al. TNF- α -mediated m(6)A modification of ELMO1 triggers directional migration of mesenchymal stem cell in ankylosing spondylitis. *Nat Commun* 2021;12:5373.
- [42] Yuan Y, Zhu C, Wang Y, Sun J, Feng J, Ma Z, et al. α -Ketoglutaric acid ameliorates hyperglycemia in diabetes by inhibiting hepatic gluconeogenesis via serpin1e signaling. *Sci Adv* 2022;8:eabn2879.
- [43] Nury H, Dahout-Gonzalez C, Trézéguet V, Lauquin GJ, Brandolin G, Pebay-Peyroula E. Relations between structure and function of the mitochondrial ADP/ATP carrier. *Annu Rev Biochem* 2006;75:713–41.
- [44] Jing Y, Niu Y, Liu C, Zen K, Li D. In silico identification of lipid-binding α helices of uncoupling protein 1. *Biomed Res* 2018;9:313–7.
- [45] Crichton PG, Lee Y, Kunji ER. The molecular features of uncoupling protein 1 support a conventional mitochondrial carrier-like mechanism. *Biochimie* 2017;134:35–50.
- [46] Taylor CT, Colgan SP. Hypoxia and gastrointestinal disease. *J Mol Med* 2007;85:1295–300.
- [47] Heidenreich S, Weber P, Stephanowitz H, Petricek KM, Schütte T, Oster M, et al. The glucose-sensing transcription factor ChREBP is targeted by proline hydroxylation. *J Biol Chem* 2020;295:17158–68.
- [48] Khan Z, Michalopoulos GK, Stolz DB. Peroxisomal localization of hypoxia-inducible factors and hypoxia-inducible factor regulatory hydroxylases in primary rat hepatocytes exposed to hypoxia-reoxygenation. *Am J Pathol* 2006;169:1251–69.

- [49] Barth S, Edlich F, Berchner-Pfannschmidt U, Gneuss S, Jahreis G, Hasgall PA, et al. Hypoxia-inducible factor prolyl-4-hydroxylase PHD2 protein abundance depends on integral membrane anchoring of FKBP38. *J Biol Chem* 2009;284:23046–58.
- [50] Meyer JG, Niemi NM, Pagliarini DJ, Coon JJ. Quantitative shotgun proteome analysis by direct infusion. *Nat Methods* 2020;17:1222–8.
- [51] Cheng H, Sebaa R, Malholtra N, Lacoste B, El Hankouri Z, Kirby A, et al. Naked mole-rat brown fat thermogenesis is diminished during hypoxia through a rapid decrease in UCP1. *Nat Commun* 2021;12:6801.
- [52] Mazzatti D, Lim FL, O'Hara A, Wood IS, Trayhurn P. A microarray analysis of the hypoxia-induced modulation of gene expression in human adipocytes. *Arch Physiol Biochem* 2012;118:112–20.
- [53] Han JS, Jeon YG, Oh M, Lee G, Nahmgoong H, Han SM, et al. Adipocyte HIF2 α functions as a thermostat via PKA C α regulation in beige adipocytes. *Nat Commun* 2022;13:3268.
- [54] Han JS, Lee JH, Kong J, Ji Y, Kim J, Choe SS, et al. Hypoxia restrains lipid utilization via protein kinase A and adipose triglyceride lipase downregulation through hypoxia-inducible factor. *Mol Cell Biol* 2019;39.
- [55] Betz MJ, Enerbäck S. Targeting thermogenesis in brown fat and muscle to treat obesity and metabolic disease. *Nat Rev Endocrinol* 2018;14:77–87.
- [56] Pohar AL, Veyrat-Durebex C, Altirriba J, Montet X, Colin DJ, Caillon A, et al. Ectopic UCP1 overexpression in white adipose tissue improves insulin sensitivity in *lou/C* rats, a model of obesity resistance. *Diabetes* 2015;64:3700–12.
- [57] Inokuma K, Okamatsu-Ogura Y, Omachi A, Matsushita Y, Kimura K, Yamashita H, et al. Indispensable role of mitochondrial UCP1 for antiobesity effect of beta3-adrenergic stimulation. *Am J Physiol Endocrinol Metab* 2006;290:E1014–21.
- [58] Feldmann HM, Golozoubova V, Cannon B, Nedergaard J. UCP1 ablation induces obesity and abolishes diet-induced thermogenesis in mice exempt from thermal stress by living at thermoneutrality. *Cell Metabol* 2009;9:203–9.
- [59] Luijten IHN, Feldmann HM, von Essen G, Cannon B, Nedergaard J. In the absence of UCP1-mediated diet-induced thermogenesis, obesity is augmented even in the obesity-resistant 129S mouse strain. *Am J Physiol Endocrinol Metab* 2019;316:E729–40.
- [60] Wang B, Tsakiridis EE, Zhang S, Llanos A, Desjardins EM, Yabut JM, et al. The pesticide chlorpyrifos promotes obesity by inhibiting diet-induced thermogenesis in brown adipose tissue. *Nat Commun* 2021;12:5163.
- [61] Mills EL, Harmon C, Jedrychowski MP, Xiao H, Garrity R, Tran NV, et al. UCP1 governs liver extracellular succinate and inflammatory pathogenesis. *Nat Metab* 2021;3:604–17.
- [62] Wang H, Willershäuser M, Li Y, Fromme T, Schnabl K, Bast-Habersbrunner A, et al. Uncoupling protein-1 expression does not protect mice from diet-induced obesity. *Am J Physiol Endocrinol Metab* 2021;320:E333–45.
- [63] Dieckmann S, Strohmeyer A, Willershäuser M, Maurer SF, Wurst W, Marschall S, et al. Susceptibility to diet-induced obesity at thermoneutral conditions is independent of UCP1. *Am J Physiol Endocrinol Metab* 2022;322:e85–100.
- [64] Huo Z, Ye JC, Chen J, Lin X, Zhou ZN, Xu XR, et al. Prolyl hydroxylase domain protein 2 regulates the intracellular cyclic AMP level in cardiomyocytes through its interaction with phosphodiesterase 4D. *Biochem Biophys Res Commun* 2012;427:73–9.
- [65] Inokuma K, Ogura-Okamatsu Y, Toda C, Kimura K, Yamashita H, Saito M. Uncoupling protein 1 is necessary for norepinephrine-induced glucose utilization in brown adipose tissue. *Diabetes* 2005;54:1385–91.
- [66] Lowell BB, Spiegelman BM. Towards a molecular understanding of adaptive thermogenesis. *Nature* 2000;404:652–60.
- [67] Abreu-Vieira G, Xiao C, Gavrilova O, Reitman ML. Integration of body temperature into the analysis of energy expenditure in the mouse. *Mol Metabol* 2015;4:461–70.
- [68] Appelhoff RJ, Tian YM, Raval RR, Turley H, Harris AL, Pugh CW, et al. Differential function of the prolyl hydroxylases PHD1, PHD2, and PHD3 in the regulation of hypoxia-inducible factor. *J Biol Chem* 2004;279:38458–65.
- [69] Škop V, Guo J, Liu N, Xiao C, Hall KD, Gavrilova O, et al. The metabolic cost of physical activity in mice using a physiology-based model of energy expenditure. *Mol Metabol* 2023;71:101699.
- [70] Nonogaki K, Abdallah L, Goulding EH, Bonasera SJ, Tecott LH. Hyperactivity and reduced energy cost of physical activity in serotonin 5-HT(2C) receptor mutant mice. *Diabetes* 2003;52:315–20.
- [71] Yoon H, Spinelli JB, Zaganjor E, Wong SJ, German NJ, Randall EC, et al. PHD3 Loss Promotes Exercise Capacity and Fat Oxidation in Skeletal Muscle. *Cell Metabol* 2020;32:215–228.e217.
- [72] Leinonen H, Koivisto H, Lipponen HR, Matilainen A, Salo AM, Dimova EY, et al. Null mutation in P4h-tm leads to decreased fear and anxiety and increased social behavior in mice. *Neuropharmacology* 2019;153:63–72.
- [73] Salazar MG, Cervera IP, Wang R, French K, García-Martin R, Blüher M, et al. Adipocyte-specific deletion of the oxygen-sensor PHD2 sustains elevated energy expenditure at thermoneutrality. 2021.2001.2005 bioRxiv 2021:425401.
- [74] Matsuura H, Ichiki T, Inoue E, Nomura M, Miyazaki R, Hashimoto T, et al. Prolyl hydroxylase domain protein 2 plays a critical role in diet-induced obesity and glucose intolerance. *Circulation* 2013;127:2078–87.
- [75] Jun JC, Devera R, Unnikrishnan D, Shin MK, Bevans-Fonti S, Yao Q, et al. Adipose HIF-1 α causes obesity by suppressing brown adipose tissue thermogenesis. *J Mol Med* 2017;95:287–97.
- [76] Lee YS, Kim JW, Osborne O, Oh DY, Sasik R, Schenk S, et al. Increased adipocyte O2 consumption triggers HIF-1 α , causing inflammation and insulin resistance in obesity. *Cell* 2014;157:1339–52.
- [77] Krishnan J, Danzer C, Simka T, Ukropec J, Walter KM, Kumpf S, et al. Dietary obesity-associated Hif1 α activation in adipocytes restricts fatty acid oxidation and energy expenditure via suppression of the Sirt2-NAD⁺ system. *Genes Dev* 2012;26:259–70.
- [78] Liu Y, Ma Z, Zhao C, Wang Y, Wu G, Xiao J, et al. HIF-1 α and HIF-2 α are critically involved in hypoxia-induced lipid accumulation in hepatocytes through reducing PGC-1 α -mediated fatty acid β -oxidation. *Toxicol Lett* 2014;226:117–23.
- [79] Lee DC, Sohn HA, Park ZY, Oh S, Kang YK, Lee KM, et al. A lactate-induced response to hypoxia. *Cell* 2015;161:595–609.
- [80] Kozlova N, Wottawa M, Katschinski DM, Kristiansen G, Kietzmann T. Hypoxia-inducible factor prolyl hydroxylase 2 (PHD2) is a direct regulator of epidermal growth factor receptor (EGFR) signaling in breast cancer. *Oncotarget* 2017;8:9885–98.
- [81] Klingenberg M, Huang SG. Structure and function of the uncoupling protein from brown adipose tissue. *Biochim Biophys Acta* 1999;1415:271–96.
- [82] Ruprecht JJ, Hellawell AM, Harding M, Crichton PG, McCoy AJ, Kunji ER. Structures of yeast mitochondrial ADP/ATP carriers support a domain-based alternating-access transport mechanism. *Proc Natl Acad Sci U S A* 2014;111:E426–34.
- [83] Matejkova O, Mustard KJ, Sponarova J, Flachs P, Rossmeisl M, Miksik I, et al. Possible involvement of AMP-activated protein kinase in obesity resistance induced by respiratory uncoupling in white fat. *FEBS Lett* 2004;569:245–8.
- [84] Li L, Ma L, Luo Z, Wei X, Zhao Y, Zhou C, et al. Lack of TRPV1 aggravates obesity-associated hypertension through the disturbance of mitochondrial Ca²⁺ homeostasis in brown adipose tissue. *Hypertens Res* 2022;45:789–801.